Theory of hydrogen in diamond

2003 J. Phys.: Condens. Matter 15 R551

(http://iopscience.iop.org/0953-8984/15/17/201)

INSTITUTE OF PHYSICS PUBLISHING JOURNAL OF PHYSICS: CONDENSED MATTER

J. Phys.: Condens. Matter **15** (2003) R551–R580 PII: S0953-8984(03)58537-X

TOPICAL REVIEW

Theory of hydrogen in diamond

Jonathan P Goss

School of Natural Science, University of Newcastle upon Tyne,
Newcastle upon Tyne NE1 7RU, UK

E-mail: J.P.Goss@ncl.ac.uk

Received 20 January 2003, in final form 24 February 2003
Published 22 April 2003
Online at stacks.iop.org/JPhysCM/15/R551

Abstract

Hydrogen is a ubiquitous impurity in diamond but in contrast to other group IV materials the microscopic structure adopted in bulk material has largely remained elusive. It has therefore been the role of modelling to predict the properties of H in bulk diamond, as well as the interactions with impurities and other defects. Presented here is an account of the current theoretical understanding of hydrogen in diamond.

Contents

0953-8984/03/170551+30$30.00

1. Introduction

An interest in the properties of hydrogen as an impurity in semiconductors has been driven largely by the impact that hydrogenation has on the electrical characteristics of devices, as detailed in several excellent reviews [1–8]. It is therefore of no great surprise that a particular effort has been made in the direction of hydrogen-induced effects in silicon and III–V compound semiconductors. For instance, hydrogen alters the properties of silicon in a number of key ways, particularly in the passivation of donors or acceptors, as well as the passivation of unwanted deep recombination centres such as transition metals.

In diamond the situation is very different, not least because of the relatively limited sense in which diamond is used as an electronically active material. This is, however, a situation that seems set to change. Recent developments in plasma-assisted chemical vapour deposition (CVD) techniques [9] has led to the production of material which has electron and hole mobilities of 4500 and 3800 $cm^2\ V^{-1}$, respectively, as well as long carrier lifetimes. It is therefore likely that diamond will at least fill a niche as a semiconductor material for some specialized areas where conventional materials fail. The growth in interest in CVD material, as well as an expansion in the number of research groups working on doping issues in diamond (n-type doping has been a long-standing problem), has led to an increase in the number of theoretical studies involving the role of hydrogen.

Experimentally there are data which are correlated with the presence of hydrogen. It is known that diamonds are always contaminated with hydrogen, with total concentration as high as 1 at. % in some natural [10] and polycrystalline CVD [11] diamonds. Direct experimental techniques for the observation of hydrogen include infrared (IR) absorption, electron paramagnetic resonance (EPR) and optical measurements, but the conclusive assignment of these spectra to specific hydrogen related structures in the diamond remains to be achieved. Perhaps the only *unambiguous* data on the atomic scale at this time are that from muon spin rotation (μSR), where the local structure of muonium is taken to be also that adopted by interstitial hydrogen [12]. Muonium can be viewed as a light isotope of hydrogen, and where H is observed directly, such as in silicon and germanium, muonium and hydrogen resemble each other rather closely. In diamond muonium is found in at least two states, as is the case in silicon [13] and germanium [14]: normal muonium possesses an isotropic spectrum, and is assigned to muonium at or about the tetrahedral interstitial site, whereas anomalous muonium (Mu^*) is axially symmetric and is located at a bond-centred site (see figure 1). Simple theoretical considerations [15] that seem to work for muonium in Si and Ge failed for diamond [12]. Thermalization data also showed differences between diamond and the other group IV materials, in that the Mu^* defect is distinctly more stable.

EPR experiments, which only detect defects with unpaired electrons, performed on CVD films commonly detect the H1 centre [16–21]. This defect is stable up to $\sim$1500 °C [20], has been correlated with grain boundaries [22] and is believed to be electrically active [20]

with a level around 1 eV above the valence band [23]. Recently the symmetry of H1 has been established to be 'nearly' trigonal [24], which seems to support the notion of a H-vacancy complex. Other hydrogen-related EPR has also been detected, such as the H2 EPR centre which occurs alongside H1 [20], and several others have recently been assigned to di-vacancy–hydrogen complexes [25]. The H1 and H2 centres have been interpreted in terms of a hydrogen atom lying 1.9 and 2.3 Å away from a carbon dangling bond [20]. For both H1 and H2 the isotropic hyperfine coupling constants are very small ($5. \pm 2.5$ and 4.0 ± 2.0 MHz, respectively).

There are many IR absorption peaks in the range expected for C–H stretching modes (2750–3300 cm^{-1}) [11, 26]. None of them are particularly well understood, but are generally categorized in terms of particular types of bonding of carbon (sp^2/sp^3). A commonly detected mode in the natural material lies at 3107 cm^{-1}. The defect responsible is unlikely to be due to on-axis bond centred hydrogen, since the most straightforward interpretation of the overtone structure implies that the defect does not possess inversion symmetry [27]. Furthermore, isotopic data indicate that the centre involves only one carbon atom [28], and although stress measurements have been made, no splittings were resolved [29] so that the point group symmetry is not known. The involvement of nitrogen in this defect was ruled out because there is no significant change in its frequency with ^{15}N [28]. However, one should be careful in such an assertion, and a more precise interpretation of the experiment is that, if nitrogen is present in the defect, it is not involved in the 3107 cm^{-1} vibration. The centre can be formed and removed in natural and synthetic diamond by an appropriate high temperature annealing treatment [30, 31], suggesting a particularly stable centre. Additionally, in CVD material there is a C–H related IR absorption band which mirrors many of the characteristics of the 3107 cm^{-1} line, but is shifted upwards in frequency by 17 cm^{-1} [28]. This centre exhibits the same isotopic shifts with ^{13}C ($\sim$9 cm^{-1}), and is likely to be due to a similar atomic structure to the 3107 cm^{-1} centre.

The most clear evidence for H-related defects in diamond comes from the passivation of boron acceptors by in-diffused deuterium [32–36]. Similar experiments in n-type (nitrogen-containing) diamond did not show the same behaviour [37], perhaps indicating the influence of the Fermi level and electrical levels of hydrogen on the deuterium mobility, i.e. that positively charged hydrogen is mobile whereas neutral or negatively charged interstitial hydrogen is not.

Another role of hydrogen in diamond that has received attention in the recent past is that associated with the phenomenon of a surface conductive layer seen in hydrogenated diamond samples. Within the experimental community there are two models that describe very different mechanisms involving hydrogen. The first is that there is a subsurface defect involving hydrogen which possesses an acceptor level an order of magnitude shallower than that of boron [38–41]. Now, it is very important to remember that boron is otherwise the most shallow acceptor detected in diamond, with the acceptor level lying at $E_v + 0.37$ eV [42]. Effective mass theory places the acceptor level at [43]

$$E = \left(\frac{\varepsilon_0}{\varepsilon_{\text{diamond}}}\right)\left(\frac{m^*}{m_0}\right)E_{\text{H}},$$

where ε_0 and $\varepsilon_{\text{diamond}}$ are the permittivity of free space and diamond, respectively, m^* is the effective mass of the valence band top and $E_{\text{H}} = 13.6$ eV is the binding energy of the hydrogen atom. This yields a value close to 0.33 eV for the effective-mass acceptor in diamond[1], whereas various values from a few millielectronvolts to a few tens of millielectronvolts have been quoted for the surface conduction [46–50]. Such a shallow level is therefore difficult to explain by conventional means. The more widely accepted model for the conductivity is that of transfer

[1] $\varepsilon_{\text{diamond}}/\varepsilon_0$ is taken as 5.570 [44]. m^*/m_0 is not known very accurately, but is taken to be $\sim$0.75 [45].

doping, with an aqueous layer on the surface of the diamond effectively acting as a source of valence band holes. The role of the hydrogen in this case is believed to be simply to provide a surface with the correct electrical properties, versus a valence band maximum high enough in energy to lie above the 'acceptor level' of the species in solution [50–53]. However, it is important to acknowledge the fact that hydrogenation of diamond surfaces leads to a peak in the hydrogen concentration in a subsurface layer that may extend for several nm [32, 33, 35, 38, 54], which may passivate compensating defects and hence affect the conductivity directly.

Finally, in contrast to the rich variety of luminescent and absorption peaks associated with other impurities such as nitrogen [55] and nickel [56, 57], hydrogen is responsible for only a few optical centres for which there is relatively little unambiguous data [55, 58]. For instance, early reports of a broad green band around 540 nm being associated with hydrogen [38, 54] have been drawn into doubt by later photoluminescence excitation experiments [59]. Where there is less controversy in assignment to hydrogen is in the near-IR transitions that lie between around 0.7 and 0.9 eV [28].

The role of theory is to explain the experimental data where possible and help predict the effect that hydrogen may have on dopants and defect formation processes. In section 2 a broad description is give of the techniques that have been applied to hydrogen-related defects in diamond, along with an outline of the experimental observables that can be evaluated theoretically with a useful degree of accuracy. This is followed by an analysis of the theory of interstitial hydrogen and muonium in section 3, H–H complexes in section 4, vacancy–hydrogen complexes in section 5, H–X complexes in section 6 and extended H-related centres are briefly reviewed in section 7.

2. Theoretical approaches

The rapidly increasing availability of fast computing resources over recent years has led to a dramatic change both in the level of complexity of the atomistic/quantum mechanical models used and the size of the systems considered on a routine basis. For example, taking just the density functional approach as an example, it was not atypical twenty years ago to be modelling point defects using clusters of atoms which barely extended beyond the neighbouring atoms of the impurities, whereas now systems containing hundreds of atoms are commonplace, and even considered essential for a correct description of defect properties.

In this section, a brief description of the theory employed in the study of hydrogen in diamond will be presented. Since the theoretical frameworks are well developed and constitute a highly technical subject in their own right, it will only be possible to indicate the types of experimentally observable properties that can be calculated, and with what accuracy.

2.1. Hartree–Fock based methods

The basic problem to be solved is the quantum mechanical interaction of a many-particle system constituted from atomic nuclei and electrons. Usually the problem is first split into these two terms under the adiabatic approximation, and then one solves the electronic problem for a set of nuclear coordinates. One approach to the electron problem involves the construction of a many-body wavefunction for the system in the form of a Slater determinant. This approach is the basis of *ab initio* Hartree–Fock (HF) methods, as well as a number of derived semi-empirical approaches.

In addition to the basic assumption, one usually adds further approximations. For example, the core electrons associated with the atomic species are usually removed from the calculation by the use of pseudopotentials that explicitly consider only those electronic states involved in the bonding processes [60].

For the *ab initio* approach the size of system that can be tackled is severely limited due to the computational effort required. This is further compounded by the lack of electron correlation in HF theory, which leads the method to fail for some problems. Correlation can be included by using the configuration-interaction (CI) approach, but the associated computational costs makes this technique impractical for all but very small clusters of atoms.

To calculate the properties of larger systems one must eliminate some of the terms in the calculation. One method is the so-called partial retention of diatomic differential overlap (PRDDO) [61, 62], which can be termed an approximate *ab initio* technique. Furthermore, *parametrizing* the integrals, which can be done at several levels of sophistication, leads to a highly simplified and computationally light numerical scheme, as embodied in complete neglect of diatomic overlap (CNDO), intermediate neglect of diatomic overlap (INDO), modified neglect of diatomic overlap (MDNO) and so on [63, 64]. An important consideration is that the empirical terms are derived from various experimental parameters such as electron affinity and ionization energies of specific systems, which introduces questions of transferability.

2.2. Density functional methods

HF based methods are not currently commonly used for problems in the solid state due to the computational expense and lack of electron correlation, although it is commonly used in molecular chemistry modelling. Instead the majority of *ab initio* calculations are based in the density-functional theory (DFT). DFT was developed nearly forty years ago by Hohenberg and Kohn [65] and adapted by Kohn and Sham [66] to produce a computationally accessible formalism. Unlike HF based schemes, this approach has the electron density as the fundamental variable. There are several books and reviews regarding the details of density functional based techniques and their applications [67–71].

It is important to appreciate the general features of the method. During the calculation, typically one evaluates the charge density in terms of a set of eigenvalues and eigenfunctions which have the appearance of representing one-electron energies and wavefunctions, and often they are quoted in those terms. However, one must exercise caution in doing so. These are the so-called Kohn–Sham states.

Typically, as with the HF based methods, density functional techniques are augmented with additional approximations, each in turn required to render the solution of the many-body problem tractable. One key approximation is that of how the exchange and correlation potentials are incorporated into the calculation, leading to the local density approximation (LDA) and higher-order schemes such as the generalized gradient approximation (GGA), although exact exchange–correlation calculations can also be performed at some computational cost. As with HF based techniques, core electrons are typically removed using pseudopotentials.

2.3. Tight-binding approaches

Tight-binding (TB) methods treat a system as a set of perturbed neutral atoms, with weak atomic interactions being dealt with parametrically. These parameters can be taken from fitting to experimental or theoretical data, such as from HF or DFT, the latter leading to the DF-TB method that has been applied with great success in a range of solid state problems [72–74] (for a review see [75]). The TB methods have similar advantages to parametrized HF methods, in that they are much faster than the full *ab initio* methods, but the approach can lead to shortcomings in situations where charge transfer is important, or where the coordination of atoms differs greatly from the state used for the parametrization.

2.4. Basis sets and Brillouin zone sampling

The basis set used to represent the charge density and the eigenstates can greatly affect the calculation. Most commonly plane waves and Gaussian functions are used. The plane waves have an advantage where the geometry of the system in question is periodic, or band-like. Therefore one typically finds that models utilizing the supercell geometry expand the charge density and eigenstates in terms of these Bloch states. However, where the system is highly localized, such as in the case of molecular systems or where a defect is present in a crystal, it is perhaps more appropriate to use localized orbitals such as Gaussians. Some basis sets use a hybrid approach.

Where a periodic system is used there is a further complication. Take the case of the evaluation of the total energy of a crystalline material such as diamond. It is well known that for a perfect periodic material there is dispersion in the electron eigenstates in reciprocal space, i.e. one must consider the band structure of the material. Clearly the total energy of a primitive cell of diamond will, in general, require an integral over k-space, but in practice one can efficiently obtain such an integral by considering only a few special k-points, using schemes such as that derived by Monkhorst and Pack [76]. In this case the Brillouin zone is sampled using a uniform mesh of points that can be reduced by considering the symmetry of the system. Then for the diamond primitive unit cell which has some 48 symmetry operations associated with it, a mesh made up from $10 \times 10 \times 10$ points can be reduced by around a factor of ten.

2.5. Classical versus quantum mechanical treatment of the H atoms

Within all the preceding frameworks, it is usually taken that the motion of the nuclei can be treated classically. However, in the case of light impurities this is not necessarily true. For H in silicon a number of attempts have been made to treat the system with the zero-point motion of the proton(s) included [77–81]. In some cases on may add a correction *post hoc*, such as that shown for the hyperfine coupling of muonium in diamond (section 3.1) or the comparison of migration barriers computed using static methods with the computed vibrational modes [82]. Although this latter approach is much less rigorous than including the quantum-mechanical properties of the proton at all stages of the calculation, it is by far the most common due to the computational difficulty in a full calculation. The inclusion of the zero-point motion will in particular have an effect on migration barriers, but where it has been shown to be important, the migration barriers are relatively small. However, since the zero-point motion will in general have some effect on all the computed quantities, it is important that one interprets the computational results with this in mind.

2.6. Summary

Although the preceding paragraphs only indicate in very broad terms the approximations inherent in computational techniques, an important fact to appreciate is that there is no unique paradigm for evaluating the wavefunctions or charge density, even within a given theoretical basis such as DFT. Hence total energies and derived quantities from ostensibly the same approach may differ considerably and it is not always clear which results are the more accurate. Such cases arise in the calculation of the hyperfine terms of muonium and the location of electrical levels such as the donor level of substitutional sulfur. One must therefore always exercise caution in the interpretation of derived properties. In the next section a range of observables are described with, where possible, a guide to typical accuracies.

2.7. Calculation of experimental observables

It is usual for papers presenting the results of high level atomistic calculations to report the natural data of the methods, such as structure (bond lengths, angles, etc), energies relative to some reference, wavefunctions and charge densities. Although these parameters are of particular use when comparing modelling techniques against each other, in order to apply the theory to real problems it is imperative to develop techniques for accurately estimating experimentally obtained parameters. Currently a range of observables are calculated with reasonable accuracy in the case of defects in diamond, including optical transition energies and lifetimes [83], vibrational frequencies [84–86], magnetic parameters (A- [87], D-tensors [85]), donor and acceptor levels [88, 89], binding energies, migration [85, 90] and reorientation [91] barriers and piezospectroscopic stress tensors [92]. Below, the methods for the estimation of a selection of these important properties are outlined.

2.7.1. Formation energy and solubility. The formation energy of a system can be expressed as

$$E^f(X,q) = E^t(X,q) - \left(\sum_i \mu_i\right) + q(E_v + \mu_e) + \chi(X,q). \tag{1}$$

Here $E^f(X,q)$ is the formation energy of system X in charge state q, $E^t(X,q)$ is the total energy of system X in charge state q from the computation (DFT, etc), μ_i are the chemical potentials of the atomic species, with the sum over the atoms in the system, E_v is the energy of the valence band top, μ_e is the electron chemical potential relative to the valence band top and $\chi(X,q)$ is a correction term for terms such as charge–charge and multipole interactions that arise due to periodic boundary conditions [93], where appropriate. Thus the formation energy represents the energy required to assemble the system from its constituent parts and represents a thermodynamically significant property. The thermodynamic equilibrium solubility of X is then simply given by the usual expression [94]

$$[X] \sim N_s \exp\left(-\frac{G}{k_B T}\right), \tag{2}$$

where N_s is the site density (which includes a contribution from configurational entropy), G is the free energy of the defect, k_B is Boltzmann's constant and T is the absolute temperature. Since $G = E^f(X,q) - TS$, this includes a contribution from the vibrational entropy. Unfortunately, to the knowledge of the author, there is no published work that quantifies the vibrational entropy term, and in general it is assumed to be small and is neglected. In particular, where the formation energy is high (perhaps several electronvolts), it is very unlikely that the vibrational entropy will make a defect soluble.

The charge–charge interaction term in $\chi(X,q)$ may be considerable [95]. It has the form $q^2\alpha/L\varepsilon$, where α is a geometric term (the Madelung constant), L is the length scale of the system (typically a supercell dimension) and ε is the static dielectric constant of the medium. For a 64-atom cubic unit cell of diamond this yields $\sim 0.5q^2$ eV: for $q = 2$ this amounts to more than 2 eV! Clearly such a 'correction' may dominate the formation energy and render calculated solubilities of charged defects unreliable.

The absolute formation energy E^f is a challenging quantity to obtain accurately in any case since there is enormous uncertainty in the appropriate values for the chemical potentials of the constituent atoms μ_i in equation (1). As a relevant example, one may take μ(H) from the free atom, half the energy of a free hydrogen molecule or from some other energy considerations such as taking the formation energy of CH_4 to be zero [82, 96, 97]. Taking the atomic versus molecular systems as an example one can see that we have a problem:

experimentally the binding energy of H_2 is 4.52 eV [98], and therefore the values of μ (H atom) and μ(H molecule) *must* differ by 2.26 eV. As a consequence the formation energy of any defect containing one hydrogen impurity must also differ by this amount. Clearly, changing E^f by such an amount in equation (2) might lead to a qualitative change in the solubility. However, where the formation energy is already very large such variations in the chemical potential may make no material difference, and an estimate of the absolute formation energy, and hence the solubility, can be useful.

2.7.2. Formation energy and electrical levels. The H1 EPR centre is believed to be an example of an electrically active hydrogen-related defect in diamond. Furthermore, hydrogenation passivates boron-doped material, and the interaction of hydrogen with other impurities theoretically produces shallow donors. Therefore it is important to be able to estimate the location of electron and hole traps in the band gap. This can be achieved from first principles using equation (1). One then extracts the charge state with the minimum formation energy as a function of μ_e. Then, for instance, the donor level (often given as the (0/+) level) is given by the value of μ_e for which $E^f(X, 0) = E^f(X, +1)$. Thus, for material where the electron chemical potential (or Fermi level) lies below the (0/+) value (such as B-doped material), the defect will be positively charged. A similar method yields the acceptor level (written as $(-/0)$ level), or in fact any change in charge state.

Unlike the solubility, the electronic levels do not depend on the chemical potentials of the atoms in equation (1), since they cancel in the comparison of two charge states. However, the contribution from the correction term, χ is explicitly dependent on q, and in particular the charge–charge or Madelung correction scales as q^2. This means that electronic transitions such as (2+ /3+) will be strongly affected by χ [95]. Additionally one might choose different schemes for evaluating E_v such as from a band structure, or perhaps by estimating the ionization energy of a bulk cell. When quoting electrical levels calculated in this fashion, it is usually correct to reference them to the valence band top, as this is the term used in the computation (see equation (1)). One can reference the electrical levels to the conduction band minimum, but it is not clear whether one should use the theoretical or experimental band gap in this procedure. Where electrical levels from the literature are quoted in this review, the values and the band to which they are referenced are as found therein.

The formation energy approach for the calculation of electronic levels is widespread, but there have been notable failures. For example, the A-centre in silicon (an interstitial oxygen atom bridging two dangling bonds in a lattice vacancy) experimentally has an acceptor level at $E_c - 0.17$ eV [99], whereas theory has predicted the acceptor level to lie at $E_v + 0.4$ eV [100]. This particular problem may be in part due to the poor description of reconstructions in vacancies typically found in supercell calculations, but also the effect of dispersion in defect-related Kohn–Sham states in the periodic model, and the fundamental underestimate of the band gap in DFT also play a role.

2.7.3. Alternative strategies for calculating electrical levels. One can adopt a number of alternative strategies to estimate defect levels. The first is to use some sort of marker, such as where an empirical correction is used [101]. This eliminates systematic errors in DFT calculations where an underestimate in the band gap can strongly perturb the position of defect levels—in the case of chalcogen defects in silicon the marker approach corrected the errors found in the formation energy method [102]. This approach is only possible where reliable experimental data are available. However, one can in fact retain the *ab initio* nature of a calculation by effectively using bulk material as a marker [103]. One can then replace E_v in equation (1) by the ionization energy of a bulk system of the same size as the defect under consideration. This has an additional advantage in that the correction terms χ in equation (1)

approximately cancel. When using a marker, it is most sensible to reference the electrical level to the same band edge as the marker, so following the bulk ionization and affinity approach, donor levels are best referenced to E_v and acceptors to E_c. Of course, given the band-gap energy one can convert between these.

A less rigorous way to obtain an estimate of the donor and acceptor levels in DFT calculations is simply to assume that the Kohn–Sham levels indicate the location of the defect level. However, this can be misleading: for example a neutral defect may possess unoccupied gap levels but be unstable in the negative charge state (for example the addition of an electron may drive the previously unoccupied level above the conduction band minimum). In fact to be rigorous one *must* take into account all charge states for the evaluation of donor or acceptor levels. Having said this, the presence of Kohn–Sham gap levels in DFT calculations is often a good indicator of potential electrical activity and can certainly be used as an initial guide.

Finally, one can estimate electrical levels from total energies of atomic clusters [104]. In this approach one adopts a similar argument to that used in a supercell scheme [103], with the addition of a correction term for the confining potential of the cluster. A problem with this approach is that the charge added or removed from a hydrogen-terminated cluster may be affected in ways not described by the simple confinement of the charge, so that, for example, the charge on an ionized donor or acceptor may reside predominantly in the shells of atoms close to the surface. This said, the method has great advantages over the supercell approach from the finite nature of the system (i.e. no periodic charge–charge or multipole interactions), and real space calculations are typically computationally efficient. In particular, in the study of Albu *et al* [104] for defects where experimental data are available the overall agreement is fair, with the exception of P which is found to be too deep by a factor of two.

The problems in calculating defect levels for a wide gap material using periodic boundary conditions are perhaps less pronounced than for materials such as Si and Ge where dispersion in defect states is an appreciable fraction of the band gap. Realistically, whatever the method, the calculation of band-gap levels is probably accurate to a few tenths of an electronvolt in favourable situations, with qualitative statements such as ‘in the upper half of the band gap’, or ‘mid-gap’ being fairly secure.

2.7.4. Vibrational modes and effective charges. Local vibrational modes can act as a very clear diagnostic tool for the assignment of defect structures. Experimentally one often has data for the shifts with different isotopes and stresses, and the absolute frequency can indicate something regarding the local environment and bonding. Local modes can be detected from IR absorption, Raman scattering and as side-bands to optical transitions, and therefore constitute a key defect parameter.

Local vibrational modes (LVMs), i.e. those lying above the bulk one-phonon band, of a system can be estimated quite accurately. One method is the construction of a dynamical matrix by evaluating the energy double derivatives of the components in the system directly from total energy calculations (as in the *ab initio* approach) or by assuming some potential to describe the interactions of the atoms. Often a mixture of the two is adopted with atoms at the core of a defect being treated explicitly and the remaining atoms where the perturbation from bulk is minimal being treated using a potential [82]. Typically the energy double derivatives are obtained numerically by displacing the appropriate atoms from their equilibrium sites, although they can also be obtained analytically [105]. The dynamical matrix approach has the benefit of relative computational simplicity, but is usually within a harmonic approximation[2]. For molecular

[2] To a limited extent, energy double derivatives obtained numerically by displacing atoms include even anharmonic terms.

dynamics calculations the modes of vibration can be obtained from a statistical analysis of the motion of the atoms, which has been used, for example, for bond-centred nitrogen in diamond [106]. This approach has the advantage of implicitly including anharmonic terms in the modes of vibration, but it is computationally more difficult to obtain detailed information yielded from the dynamical matrix approach, such as isotopic effects, mode symmetries and so on.

The bond lengths and bond strengths evaluated from computations are often in error by small amounts, and as a rough guide a 3% error in a X–H bond length gives rise to a 10% error in a H-related stretch mode. Since DFT methods often *underestimate* bond lengths, one would normally expect the calculated vibrations to be overestimated. Furthermore one should be careful regarding the accuracy of harmonic approximation LVMs: since the amplitude of the H-related oscillations are often large, the contributions from anharmonicity can be large (typically several tens of cm^{-1}) [107]. Typically errors in LVMs are a few per cent, with isotopic shifts being rather more accurate in absolute terms. Therefore calculated LVMs, when combined with other evidence, may prove decisive in a defect assignment.

The integrated intensity of IR absorption due to some atomic vibration can be described by an *effective charge* of an oscillator (η). The value of η is related to the change in induced dipole during the oscillation:

$$\eta^2/m = \tfrac{1}{3}\sum(\partial M/\partial Q)^2,$$

where m is the mass of the oscillator, M is the induced dipole caused when the atoms are displaced according to their normal coordinates and Q is the amplitude of the mode. The sum is over x, y and z and over any mode degeneracy [108]. The value of η is difficult to calculate precisely, but taken as an order of magnitude guide, it can indicate if a mode of vibration should be easy or hard to detect experimentally. The effective charges of oscillations calculated this way can be viewed as being qualitative in nature, with approximately an order of magnitude agreement with experiment.

Modes that are resonant with the bulk phonons can also be examined. However, one must exercise more caution than with the local modes since the coupling of the defect vibration with bulk modes may not be modelled correctly. A Green function approach has previously been successfully applied to nitrogen defects in diamond [84], with good agreement between theory and experiment.

2.7.5. Electron paramagnetic resonance parameters. Various paramagnetic parameters can be obtained from theory. These parameters arise from an effective spin Hamiltonian and are generally characterized by the tensors g, A and for systems with an effective spin $> 1/2$, D. The hyperfine tensor, A, relates to the interaction of the electronic and nuclear spins and has been a key to the understanding of Mu and Mu^*. For an axial defect the isotropic and anisotropic components of A can be related to the measured $A_\parallel$ and $A_\perp$ by the relations $A_s = (A_\parallel + 2A_\perp)/3$ and $A_p = (A_\parallel - A_\perp)/3$ [109], where the s and p subscripts relate to atomic orbital notation. The calculation of hyperfine interaction at atom sites other than hydrogen is complicated [87] by the need for an accurate description of the system at the atomic cores, so one cannot use pseudopotentials. However, this is not an issue for H or muonium since clearly there are no core electrons in these cases. The accuracy with which hyperfine coupling terms can be estimated depends on the level of theory, and in particular the accuracy with which the wavefunctions and spin density are modelled at the hydrogen atom sites. Additionally, the fact that H defects possess large zero-point motions complicates the calculations, and averages must be taken over the likely oscillations of the atoms involved. Typically, HF methods yield fair results, with the inclusion of correlation via CI being a distinct improvement. DFT Green-

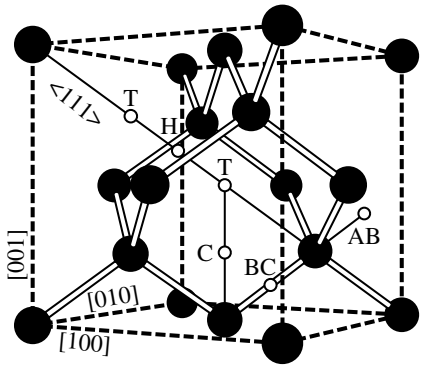

Figure 1. An illustration of the most important interstitial sites in diamond structure materials. C atoms are shown as black circles, and ideal interstitial sites as small white circles. The T site lies equidistant from four carbon sites and possesses T_d symmetry, the H site lies midway between two T sites and possesses D_{3d} symmetry, the C site is midway between an atom site and a T site along $\langle 001 \rangle$ (C_{2v} symmetry) and the bond-centred (BC) site is the mid-point between two atom sites (D_{3d} symmetry). The anti-bonded (AB) configuration is less well specified, and is usually taken to mean somewhere between an atom site and a T site along $\langle 111 \rangle$ and possesses C_{3v} symmetry.

function methods also yield very close agreement with experiment and have the advantage of a smaller relative computational effort.

One can also calculate *g*-tensors [110–112] and, for defects with effective spins of unity or greater, there is an additional term relating to the interactions between electronic spins, labelled *D* [82]. Since no calculations of these types have been applied to H in diamond, no further discussion of these tensors will be given here.

3. Muonium and interstitial hydrogen

Since there is no experimental data pertaining to isolated interstitial hydrogen in diamond, unlike other group IV materials [13, 14, 113], the data derived for muonium has been used [12]. Muons are, at least at the chemical level, a light isotope of hydrogen with a rest mass of around a ninth that of a proton. In fact, the earliest theoretical data relevant to the location and structure of interstitial hydrogen in diamond were those of the hyperfine interaction terms for the muon [114] using HF cluster techniques. However this and other early theoretical works only considered non-bonded configurations, i.e. locations such as the tetrahedral and hexagonal interstitial sites (figure 1), and locations in between [114–116], and hence Mu and Mu^* were thought to correspond to these configurations.

Theoretically, the energy of hydrogen in the various sites in diamond varies considerably. Table 1 lists the energies of hydrogen at the H, T and BC sites shown in figure 1. In particular, the relative energies of the T and BC sites vary between as little as 0.5 eV and as high as 2.7 eV, with energies in the 1–2 eV range arising from *ab initio* calculations being perhaps the most reliable.

The first proposal of a bond-centred configuration came from Cox and Symons [126] which was subsequently put on a firmer theoretical basis by Claxton *et al* [117] and Estle *et al* [118]. These early studies were unable to perform exhaustive relaxations due to the computational expense, but showed that the bond-centred site was in fact lower in energy than the cage sites, and consistent with the negative hyperfine coupling constant that had up to then been a major problem. In order to form a stable bond-centred muonium or hydrogen centre, the neighbouring carbon atoms are pushed apart such that the C–C bond is around 40% larger

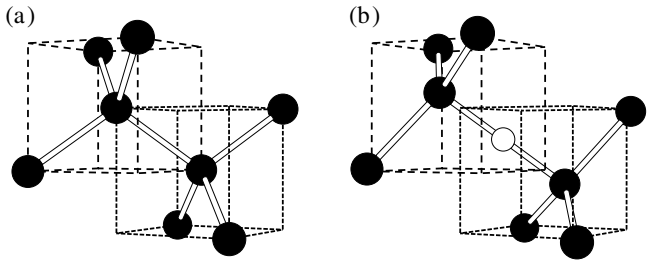

Figure 2. A schematic representation of the on-axis bond-centred structure of interstitial hydrogen and muonium in diamond: black and white circles represent carbon and hydrogen, respectively. (a) Bulk diamond centred on a bond, (b) bond-centred hydrogen including dilation of the C–C bond. The broken lines show the cubic axes with vertices located on diamond tetrahedra to emphasize the distortion shown in (b).

Table 1. Relative energies of interstitial sites for hydrogen in diamond (eV). The interstitial sites are depicted in figure 1. In each case the zero of energy is taken to be the lowest energy structure available in the relevant work.

T	H	BC	Method
0.00	0.83	—	HF, $C_{10}H_{16}$ cluster [114]
0.59	0.00	—	CNDO, $C_{30}C^{*}_{40}$ [115]
∼2.4	—	0.00	HF $C_{10}H_{16}$ cluster, estimates from figure 3, [117]
2.0	—	0.0	PRDDO, various clusters [118]
2.40	3.52	0.00	PRDDO and *ab initio* HF, various clusters [116, 119]
2.7	—	0.0	PRDDO $C_{44}H_{42}$ cluster [120]
1.9	—	0.0	LDA-DFT $C_{26}H_{30}$ cluster [121]
1.6	—	0.0	Density functional based TB 64-atom supercell [122]
0.5	—	0.0	TB 64-atom supercell [123]
1.17	1.94	0.00	LDA-DFT cluster and supercell [124]
1.0	1.7	0.0	LDA-DFT cluster and supercell [82]
0.95	1.52	0.00	LDA-DFT, 64 atom supercell [125]

than in diamond. This dilation is shown schematically in figure 2. The considerable strain energy associated with such a dilation must therefore be offset by the chemical interaction of the impurity with the host lattice. From a computational viewpoint, the large perturbation of the immediate surroundings might be thought to have an effect in the early calculations, where clusters as small as eight carbon atoms were used. It is only due to the relatively short range of the effect (the displacement of the second shell atoms is typically less than 5% of a C–C bond length) that these results were as good as they were. Table 2 lists the C–H bond lengths for bond-centred hydrogen in diamond for the various computational schemes. One should note in particular the broad consistency of the dilation with different computational schemes, with values ranging from 39 to 52%. It is noted that an approximately bond-centred site was found using TB techniques where the hydrogen atom lies closer to one of the carbon neighbours (C–H $\sim$ 0.77 Å) and off the [111] axis [123]. This structure was labelled the equilateral triangle (ET) model due to the two sets of three equivalent sites around the C–C bond that the H atom could adopt. The distance of the hydrogen atom to the further of the carbon neighbours was 1.8 Å, which is close to the estimated distance for the H1 EPR centre, for which an assignment was then made. The ET site was predicted to be 1.4 eV lower in energy than the on-site defect, but later *ab initio* calculations showed that this site was either higher in energy [132] or unstable [82], and it seems likely that the ET structure is a result of the TB parametrization.

Table 2. Structural parameters for D_{3d} bond-centred muonium or hydrogen in diamond.

C–H (Å)	C–C dilation (%)	Method
∼1.07	39	HF, $C_{10}H_{16}$ cluster [117]
1.09	41	PRDDO, $C_{44}H_{42}$ cluster [118]
1.10	42	PRDDO, $C_{44}H_{42}$ cluster [120, 127]
1.1	43	LDA-DFT, $C_{26}H_{30}$ cluster [121]
1.155	50	HF, C_8H_{18} cluster [128]
1.1	∼42	HF, C_8H_{18} cluster [129]
1.106	43.5	Semi-empirical molecular orbitals, $C_{46}H_{48}$ cluster [130]
1.05	41.3	CI, C_8H_{18} cluster [131]
1.17	52	DF-TB 64-atom supercell [122]
1.17	52	TB 64-atom supercell [123]
1.13	47	LDA-DFT, various clusters and supercells [82]
1.10	42	Hybrid-DFT, $C_{44}H_{42}$ clusters [104]
1.13	47	LDA-DFT, 64 atom supercell [125]

In both the positive and negative charge states, in contrast to silicon, hydrogen lies in the bond-centred site [82, 124, 130]. Semi-empirical methods place the H atom on-axis in all charge states, whereas both LDA-DFT and GGA-DFT place the positive charge state in a buckled bond-centred configuration [82, 89, 124] with ∼100° bond angle [82, 124]. This off-axis configuration was calculated to lie 0.24 eV lower in energy than on-axis, with no appreciable barrier to precession about the bond [82]. The puckered bond structure allows the C atoms to relax towards each other relative to the neutral charge state with a dilation of around just 21% [82]. The charged systems are, of course, diamagnetic and if the muonium counterpart can adopt these charge states, it would then not be measured in the μSR experiments.

3.1. Muonium hyperfine coupling constants

The spin density associated with muonium at the tetrahedral or bond-centred sites can be interpreted in terms of the hyperfine constants measured experimentally. In fact the hyperfine coupling data was the key determining the bond-centred site for Mu* [117, 126]. The experimental hyperfine constants for Mu and Mu* are given in table 3. Commonly the isotropic hyperfine coupling constant of normal muonium is given as a fraction of the vacuum value, denoted f.

The interaction of Mu with the host can be understood in terms of a vibrational average over the cavity [114] with the unpaired wavefunction possessing a node between the muon and the nearest neighbours [119]. The anisotropy and sign of the hyperfine coupling for Mu* arises due to the strong polarization of the valence electrons [133]: the gap state is p-like in character and nodal at the muon site [121, 129, 133] and cannot give rise to the s component seen experimentally.

The difficulty in accurately obtaining the hyperfine coupling terms arises from the sensitivity these values have to the spin density at the muon site and the effects of the zero-point motion of the muon itself. As mentioned in section 2 HF calculations do not include electron correlation, and it was suggested that this is the source of much of the error in early estimates of the hyperfine constants of anomalous muonium [120]. This appears to be borne out by the high level CI calculations [131], which yielded particularly good agreement with experiment. This suggests that the agreement of the HF calculations of Bendazzoli and Donzelli [128] was

Table 3. Hyperfine coupling constants for Mu and Mu* in diamond (MHz). A_s and A_p are the isotropic and anisotropic contributions. The (isotropic) hyperfine constant for muonium in vacuum is 4463 MHz.

Mu		Mu*		
A	f	A_s	A_p	
3347	0.75	—	—	HF [114]
5445–6337	1.22–1.42	—	—	PRDDO and HF [119]
—	—	−714 to −981	—	PRDDO, HF [120]
—	—	−136.4 to −137.4	214.6–186.5	LDA-DT Green-function [133]
—	—	−1030	130	HF [129]
—	—	−231.0	178.0	HF (vib. av.) [128]
—	—	−851	320	HF [131]
—	—	−215	280	CI [131]
—	—	−145	194	CI (vib. av.) [131]
—	—	−384	303	QDPT(S) [134]
—	—	−233	204	QDPT(S) (vib. av.) [134]
3711	0.831	−205.7	186.6	Experiment [12, 109]

fortuitous. The zero-point motion of the muon reduces the isotropic component by around a third [131] and therefore cannot be neglected.

The overall qualitative agreement for the hyperfine terms is very strong evidence for the bond-centred muonium model for Mu*, and the broad agreement between the calculated and experimental values indicates the usefulness of such calculations for other paramagnetic centres such as H1 and H2.

3.2. Electrical activity of isolated hydrogen

Due to the absence of any unambiguous data pertaining to the electrical activity of hydrogen in bulk diamond, it is instructive to briefly review what is believed to be the case for silicon. In fact the assignment of the electrical levels of single interstitial hydrogen in silicon has been controversial [101, 135–138] but, as with many other materials [138, 139], the various charge states of hydrogen correspond to different geometries and produce so-called negative-U centres. The negative charge state is either non-bonded or weakly anti-bonded to a Si atom and is highly mobile, whereas the neutral and positive charge states are located at a Si–Si bond centre. The donor and acceptor levels of bond-centred and T-site hydrogen have been calculated to lie around 0.2 eV below the conduction band and mid-gap, respectively [101, 135], with the acceptor levels being measured at $E_c - 0.56$ eV from μSR [137].

Bond-centred interstitial hydrogen in diamond has also been calculated to possess a donor level. The location of the donor level can be estimated from the location of the partially filled orbital (see section 2.7.3). However, the location of the partially filled level varies considerably, depending on the method and size of the system. For instance, the early calculation of Hoshiharu *et al* [133] placed the occupied level around 1.2 eV above the valence band top, whereas others placed it in the upper half of the band gap [121]. Similarly, a calculation of the density of states for the ET structure yielded a deep donor level around 0.5 eV above the middle of the band gap [123].

Comparison of the ionization energy and electron affinity of bond-centred hydrogen with P and B, respectively, place the donor and acceptor levels at $E_c - 3$ eV and $E_c - 1.8$ eV, respectively [82, 124]. These values are in qualitative agreement with Kohn–Sham levels [82], but the differences are not negligible: the bond-centred defect filled spin-up and empty spin-down orbitals in the neutral charge state at around $E_c - 2.0$ eV and $E_c - 1.2$ eV, respectively.

Table 4. LVMs of bond-centred hydrogen in the positive, neutral and negative charge states in diamond (cm^{-1}) from [82]. Frequencies for deuterium follow those for hydrogen in parentheses. The puckered bond-centred configuration of the positive charge state has C_s symmetry.

1+		0		1−	
Mode	Symmetry	Mode	Symmetry	Mode	Symmetry
2456 (1797)	A′	2919 (2084)	A_{2u}	2730 (1952)	A_{2u}
2086 (1598)	A′	—	—	—	—

The formation energy calculation (section 2.7.2) has been applied using DFT methods yielding various donor levels at E_v + 2.6 eV [82] and E_v + 1.2 eV [89], and acceptor levels at E_c − 2.3 eV [82] and E_v + 3.0 eV [89]. Nishimatsu *et al* [140] also list electrical levels for hydrogen in a number of locations. It is not clear how they are calculated, although the terminology indicates that they simply refer to the Kohn–Sham eigenvalues. The donor level of the bond-centred hydrogen then lies at E_v + 1.50 eV, with the T and H sites having gap levels higher in energy.

Finally, using total energy differences in cluster calculations with a quantum confinement correction yields a donor level of E_c − 3.8 eV [104], which agrees well with the previous calculations. However, the relaxation was constrained to axial symmetry, which might lead to a donor level higher in the gap than if an off-axis relaxation were permitted.

Due to the wide ranging estimates of the electronic levels, the broad conclusion is that bond-centred hydrogen possesses a donor level in the lower part of the band gap and an acceptor level at or above mid-gap. This has implications for both n- and p-type material—in the former bond-centred H will be negatively charged and compensate the donor, whereas in the latter the hydrogen will be positively charged, but still compensating the dopant. The latter case is, of course, what is seen experimentally for B-doped diamond.

3.3. Vibrational modes of interstitial H

The ideal point group symmetry of bond-centred hydrogen or muonium is D_{3d} and the irreducible representation of the stretching mode along the trigonal axis is A_{2u}. This mode is IR- but not Raman-active and has been detected at 1998 cm^{-1} for the positive charge state in silicon [141, 142]. Using just an estimate of the C–H bend and stretch spring constants, Briddon *et al* [84, 121] estimated a stretching mode at 3132 cm^{-1} for diamond, with a bend mode below the Raman frequency.

A more comprehensive set of modes was calculated also within the harmonic approximation by the LDA-DFT method [82]. These were evaluated by evaluating the dynamical matrix elements for all the atoms involved in the vibrations and are listed in table 4. The lower frequency calculated when including the motion of all atoms is unsurprising, and the frequency lies well within the range seen experimentally for C–H stretch modes in diamond.

The calculated effective charges of the vibrational modes of bond-centred hydrogen in the positive and neutral charge state are very small [82] and this suggests that large quantities could be present in the material without giving rise to any characteristic IR absorption. The effective charge in the negative charge state is much larger, perhaps suggesting that bond-centred hydrogen would be most readily visible in n-type material, should it be present.

3.4. Diffusion of interstitial hydrogen

Hydrogen in silicon can be considered to be a highly mobile species [143]. The diffusion processes are therefore subject to quantum mechanical effects that are neglected in the

Table 5. Hydrogen migration barrier heights (eV).

BC → T	T → BC	BC → C	T → H	Method
∼5.4	∼2	—	—	HF cluster [117]
5.1	2.4	—	2.5	PRDDO cluster [120, 144]
5.3	—	1.9	—	Semi-empirical cluster [130]
2.0	0.4	2.6	—	DF-TB supercell [122]
1.6	—	1.8	0.8	LDA-DFT cluster and supercell [82, 124]

estimation of migration barriers using static minimization techniques. The role of dynamic effects in the migration of the hydrogen molecule in silicon suggests that static minimization methods may well give erroneous results [81] but it seems likely that migration processes with large energy barriers are less strongly affected than the low energy processes in silicon. From a practical standpoint, the inclusion of dynamic effects is computationally expensive and, given the general agreement in many cases between static barriers and experiment, most studies tend not to include them. This is certainly the case for the current literature on the migration of hydrogen in diamond.

There are a number of possible migration trajectories for bond-centred hydrogen, and different theoretical studies have indicated qualitatively different expectations. The most simple are processes that involve only metastable or symmetry defined structures, such as BC → T and BC → H. There is then the possibility that the hydrogen atom would migrate many steps along the open channels via T → H → T hops, if it is energetically favourable. An alternative path [130] moves the H atom from the bond centre to a C_{2v} symmetry site close to the C site in figure 1.

The earliest estimates for the migration of hydrogen are those of Claxton *et al* [117] and Estle *et al* [120]. There is no directly available value from [117], but one can obtain an estimate by examination of figure 3 of that paper, where the T → BC process has a barrier of ∼2 eV. The reverse barrier is ∼5.4 eV, obtained via this value in conjunction with the data in table 1. These values agree rather well with the more formal barriers of 2.4 and 5.1 eV from [120] which used a similar computational approach. Table 5 lists migration barriers calculated for neutral interstitial hydrogen. It should be noted that the ET model has a barrier of just 0.9 eV, but since *ab initio* calculations do not support this structure [82, 89, 132], this barrier height must also be in question.

The migration of charged species is of great significance since an applied field, for example, might then greatly affect the diffusion of the species. Semi-empirical cluster calculations [145] predicted that the hydrogen interstitial lies at the bond centre in the positive and negative charge states with the barriers to migration via a structure close to the C site (figure 1) of less than 0.1 and around 2.5 eV, respectively. Therefore the migration of hydrogen is likely to take place at low temperatures in the positive charge state, such as where [B] > [H]. This was qualitatively confirmed by LDA-DFT calculations that yielded 2.0 and 0.2 eV for the negative and positive charge states, respectively [82, 124]. Noting that the zero-point energy of the bond-centred hydrogen (table 4) is comparable to the diffusion barrier one must conclude that quantum mechanical tunnelling effects, neglected in the calculation of the barrier, would be important and the conclusion can only be that the barrier is small for the positively charged defect.

It is interesting to note that one can interpret the experimental data from boron-doped diamond that the activation for deuterium migration is around 0.35 eV in the positive charge state and 1.41 eV in the neutral charge state [33, 35], so that at least the trend in mobility has been confirmed by theory.

3.5. Solubility of bond-centred hydrogen

To estimate the solubility using equation (2) one requires an absolute formation energy, with the usual caveat regarding the chemical potentials of the species (section 2.7.1). Chu and Estreicher [144], using the PRDDO approximate HF cluster technique, calculated that the energy of a H atom outside the cluster was 5.10 eV *lower* in energy than hydrogen at its most stable site in the diamond lattice versus the dilated bond centre. Thus, taking $\mu(\mathrm{H})$ in equation (1) as the energy of atomic hydrogen implies $E^f(\mathrm{H_{BC}}) = 5.1$ eV. Since N_s, in this case being the density of bond centres, is approximately 4×10^{23} cm^{-3}, even at 2000 K, the equilibrium concentration is just 10^{10} cm^{-3}. Semi-empirical molecular orbital cluster methods [130] yielded an energy difference of only ∼1.7 eV, a factor of three smaller, but this still represents a low equilibrium concentration below ∼1000 K.

Using GGA-DFT supercell techniques and the method described in section 2.7.1 the formation energy of bond-centred hydrogen is given as $\sim 2.6 + \Delta\mu(\mathrm{H})$ eV, where $\Delta\mu(\mathrm{H}) = \mu(\mathrm{H^{atom}}) - \mu(\mathrm{H^{ref}})$ is the difference between the energy of the H atom and the H reference state. LDA-DFT and GGA-DFT calculations also estimated the absolute formation energy of neutral bond-centred hydrogen to be 2.6 eV [82] and 2.7 eV [89], respectively, when compared to atomic hydrogen. A formation energy of 2.6–2.7 eV represents low equilibrium concentrations at 1000 K (equation (2) and yields [H] $\sim 10^{10}$ cm^{-3}) and hence no measurable quantity would be incorporated under equilibrium conditions at the CVD growth temperature. Of course, there are potentially temperature-dependent terms in $\mu(\mathrm{H})$, as described in various theoretical works [82, 146, 147], but these contributions are typically small even at 1000 K.

The absolute formation energy is lower in the ionized states and with the hydrogen atom as a reference state the formation energy of $\mathrm{H^+}$ is relatively small [82] when the Fermi level is close to the valence band top (i.e. p-type diamond). The concentration of interstitial hydrogen in the charged states might then be limited by the concentration of the acceptors (e.g. boron) or donors (e.g. phosphorus). This is broadly consistent with the fact that large concentrations of deuterium, close to the values of boron acceptors, can be diffused into diamond samples [32] whereas the N-doped samples, where the theoretical solubility of hydrogen is much smaller, show no such effect [37].

In summary, the consistency from three independent DFT calculations yielding a formation energy of neutral bond-centred hydrogen at around 2.6–2.7 eV relative to the hydrogen atom suggests a zero equilibrium solubility even at the high temperatures involved in diamond synthesis. However, one must bear in mind that the very act of CVD is non-equilibrium and it is clear that defects can be formed in this material in non-equilibrium concentrations, as evidenced by the presence of the H1 and H2 EPR centres.

3.6. Hydrogen in near-surface region

The phenomenon of surface conduction in hydrogenated diamond has been attributed at least in part to the role of subsurface hydrogen. This might take the passive form of removing dangling bonds by forming stable and inert C–H centres, or possibly due to the formation of an electrically active defect with shallow acceptor states. As outlined in the introduction, the current consensus is that the surface conductivity is due to surface adsorbates, but the fact remains that large concentrations of hydrogen can be found in the immediate subsurface region. In the light of the large formation energy of hydrogen point defects, this poses a significant question: what is the form of the subsurface hydrogen?

In GGA-DFT supercell calculations [132], the effect on the energy of bond-centred hydrogen in proximity to a C(100)2 × 1 surface was found with and without the presence

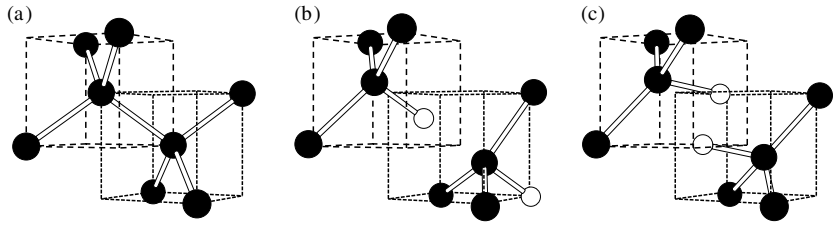

Figure 3. A schematic representation of (b) the H_2^* defect and (c) the di-bond-centred defect. (a) Bulk diamond centred on a bond. The format follows that of figure 2.

of surface dangling bonds. They calculated a BC to BC migration barrier of 2.14 eV in bulk diamond using an unstipulated trajectory, which dropped to around 1.5 eV close to the surface. There is no direct statement in this study regarding the formation energy for subsurface hydrogen, but the presence of surface dangling bonds almost removes any barrier to the motion of hydrogen toward the surface site [132]. Perhaps this is a reflection of a charge transfer from the H interstitial to the surface dangling bond and therefore the more mobile species is, in fact, H^+. Unfortunately no information was presented regarding the location of electronic states.

Despite the enhanced mobility of hydrogen in the subsurface region, the calculations still imply that hydrogen is thermodynamically unstable in diamond, and that the driving force is to remove the hydrogen from solution. However, this study only considered the role of *isolated* hydrogen, and the formation of bound complexes are likely to be important.

4. Di-hydrogen aggregates

Hydrogen is known to form dimers in Si, either taking the form of molecules [148, 149] or a metastable form termed H_2^*, shown in figure 3, made up from a bond-centred hydrogen with a close-by anti-bonded hydrogen atom forming an axially symmetric defect [150]. These have been detected via their IR characteristics, although the detection and identification of the hydrogen molecule proved to be a considerable challenge.

Mainwood and Stoneham [115] calculated the barrier to migration of the hydrogen molecule in diamond to be 0.37 eV using CNDO cluster calculations. They found that the most stable site for the molecule was centred at the T site and aligned along [001], with a barrier to rotation of 43 meV, and was less stable than atomic hydrogen in diamond by 0.14 eV. They did not consider any alternative structures for a pair of hydrogen atoms.

Although the molecule is generally found to be stable in the interstitial cages, the H_2^* configuration (figure 3(b)) has been calculated to be 3.32 eV [121], 2.23 eV [127] and 2.1 eV [82] lower in energy. The 'bond-centred' hydrogen atom becomes more closely bound to one of its carbon neighbours [127, 130]. The aggregation of hydrogen into the H_2^* configuration lowers the energy of the gap state [82, 121, 130], since one is effectively forming a fully coordinated defect (i.e. both hydrogen atoms are monovalent, unlike the isolated bond-centred defect, and all C atoms are four-fold coordinated). Various values have been calculated for the binding energy of the H_2^* pair relative to two bond-centred H defects: 1.5 eV [130] and 2.5 eV [82, 124]. The relatively large binding energy is consistent with experimental evidence for self-trapping of hydrogen in diamond [151]. Furthermore, the migration barrier for the hydrogen pair is estimated to be at least 3.5 eV [82, 124], and therefore H_2^* constitutes a very stable defect in diamond.

Just as with isolated bond-centred hydrogen, the hydrogen dimers have a large formation energy—placing a hydrogen molecule at the T site in diamond is 12.88 eV higher in energy

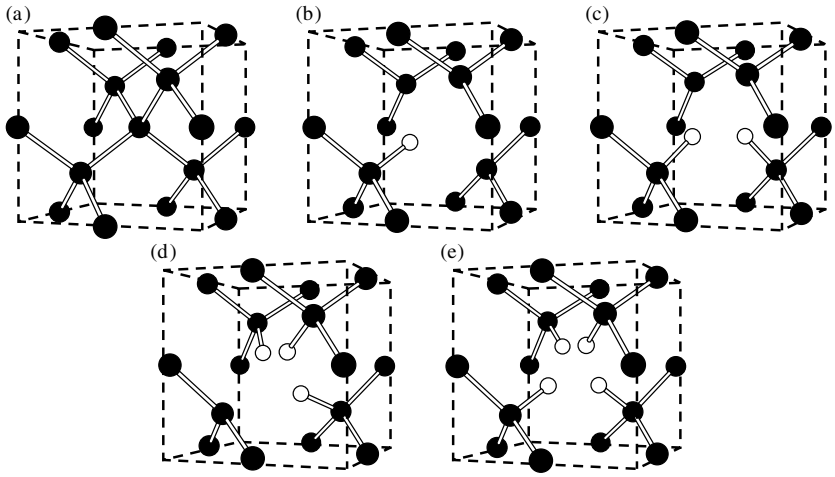

Figure 4. Schematic diagrams of (b) VH, (c) VH_2, (d) VH_3, and (e) VH_4. The black and white atoms represent carbon and hydrogen, respectively. (a) shows the corresponding section of defect-free material for comparison.

than in the gas phase [127]. Even with the energy lowering effect of forming H_2^*, and taking atomic hydrogen as the reference state of hydrogen, the solubility is practically zero.

An alternative structure can be made from placing two hydrogen atoms in the same dilated C–C bond, with the H atoms lying off-axis, as shown schematically in figure 3(c). Saada *et al* [123] found using TB methods that this structure is 2.5 eV *lower* in energy than H_2^*. However, *ab initio* LDA-DFT calculations [82, 124] do not support this assertion and placed H_2^* 0.8 eV lower in energy than the di-bond-centred configuration, which in turn was 1.3 eV lower in energy than the molecule at the T site. These calculations suggest that it is only in the positive charge state that the di-bond-centred model is comparable in energy to H_2^* [82, 124], and it is not at all clear that either defect actually possesses a donor level in the band gap [82] for the positive charge state to be stable.

The LVMs of H_2^* have been calculated to lie at 1782 cm^{-1} (E), 3511 cm^{-1}(A_1) and 3882 cm^{-1} (A_1) [82, 124]. As with the bond-centred interstitial H defect, these oscillations are believed to possess very small effective charges [82, 124], rendering them difficult to detect via infrared absorption. Combining this with the lack of electrical activity and immobility, this defect might constitute an electrically, magnetically and optically inactive reservoir of hydrogen in diamond, and hence a potential component of the large subsurface hydrogen concentration if it were not for the very low equilibrium solubility.

5. Hydrogenated lattice vacancies

It has been established from IR [152, 153], EPR [154, 155] and theoretical [156–160] studies that hydrogen binds with lattice vacancies in silicon, with a simple chemical explanation for their stability. For silicon it is believed that one can saturate all dangling bonds with hydrogen, but this may not be the case in diamond where the confined space may lead to the interaction of hydrogen atoms with each other sufficiently strongly to prevent full saturation of the dangling bonds. Figure 4 shows the structures for a lattice vacancy complexed with one to four hydrogen atoms. Mehandru and Anderson [130] found using semi-empirical cluster methods that there was a binding energy for one to four H atoms in a lattice vacancy, with the incremental binding

energy decreasing approximately linearly from 5.3 eV for the first to 2.5 eV for the fourth H atom. They also showed that the hydrogen would pin a vacancy, i.e. it would become less mobile than an isolated vacancy. However, it should be pointed out that the calculations were all carried out under the assumption of neutral systems, which is unlikely to be the case. For example, VH_1 and VH_2 are isoelectronic with the well known VN and VN_2 defects which are known to be deep acceptors [161, 162] (remember that bond-centred hydrogen is thought to be a deep donor). The strong binding of the second hydrogen atom was not reproduced in more recent semi-empirical cluster calculations, where it was found that VH_2 was 2.7 eV less stable than VH [20].

Initial work [17] suggested that the H1 EPR centre was a hydrogenated vacancy. From HF cluster calculations the separation between the H atom in the VH complex and the C dangling bonds is close to the 1.9 Å predicted for the H1 EPR centre [20]. Furthermore, despite the inherent difficulty in calculating the hyperfine coupling constants in these defects, the values from a range of methods are consistent with those of both H1 and H2, suggesting that these centres are closely related to the hydrogenated vacancies or vacancy-like structures in the vicinity of grain boundaries. Furthermore, the near-trigonal symmetry [24] points towards the VH_1 defect in figure 4. The overall experimental evidence seems to favour a location close to grain boundaries, but this does not preclude a VH complex.

The absolute formation energies for VH_n lie between about 3 eV for $n = 1$ to large negative values for $n = 4$ when μ(H) is taken from the free atom [163]. Of course this means that, in the presence of large concentrations of atomic hydrogen, and provided that thermodynamic equilibrium is achieved, diamond is unstable. If one takes perhaps a more reasonable value of μ(H) from the criterion that methane forms with zero energy, the formation energy is close to 6 eV, independent of n [163]. Under these conditions the solubility of vacancy–hydrogen complexes is zero, but of course they may form in non-equilibrium concentrations, as is the case for VN, or may be formed under proton implantation.

6. Complexes of hydrogen with impurities

6.1. Hydrogen–boron complexes

It is well established that hydrogen passivates both dopants and deep centres in commercial materials such as silicon, GaAs and GaN. The interaction of hydrogen with impurities in diamond is less clear except for the case of the passivation of boron acceptors, as outlined in section 1.

In silicon, as in most materials, hydrogen complexes with impurities by bonding either to the impurity atom itself or to a host atom that neighbours it. Four commonly adopted structures are indicated schematically in figure 5. Passivated boron in silicon adopts a structure with hydrogen in the bond-centred location [164, 165], but for diamond there is no direct experimental data to establish the site of the hydrogen atom. LDA-DFT cluster calculations [166] showed that the hydrogen lies along close to [001] from the B site, this configuration being around 0.7 eV below the H in the bond centre. Semi-empirical cluster calculations [145] suggest that the H atom is in a puckered bond-centred location such that $\angle$BHC = 113°. However, the H atom lying along [001] was only around 0.2 eV higher in energy, as was an axially symmetric bond-centred location. These small energy differences may be interpreted in terms of a low migration barrier of hydrogen in the vicinity of boron [145]. In fact these two pictures are not inconsistent: the charge density between the hydrogen, boron and the carbon nearest to H show that there are bonding interactions between all three constituents [82]. Thus the hydrogenated boron defect in diamond possesses a rather complex

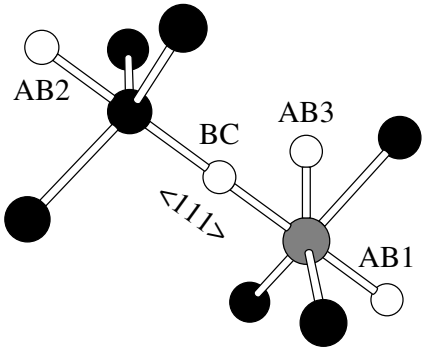

Figure 5. A schematic representation of four possible locations of hydrogen in impurity–hydrogen complexes. BC and AB refer to bond-centred and anti-bonding sites, respectively. The black, white and grey atoms represent carbon, hydrogen and impurity sites, respectively.

bonding that cannot be categorized in terms of simple covalent terms, which is typical of boron hydrides such as B_2H_6.

The hydrogenated boron centre is isoelectronic with bulk diamond [145] and there are no gap states [82]. Thus, theory confirms the experimental observation of hydrogen/deuterium passivation of p-type diamond.

Experimentally, the stability of the passivated boron is relatively high, with an experimentally estimated binding energy of 2 eV [35]. The binding energy of the B–H pair has been estimated relative to neutral bond-centred hydrogen and boron to be around 3.24 eV [145], although the actual binding energy is more likely to be related to the ionized species, calculated to be around 1.6 eV [82, 124]. The barrier to dissociation of the B–H pair has been estimated at around 1.8 eV [82, 124], which is broadly in line with experimental estimates.

The modes of vibration of the B–H pair is complicated by the proximity of equivalent total energy minima. However, a mode of around 2540–2655 cm^{-1} was obtained from LDA-DFT cluster calculations [166] and 2664 cm^{-1} from LDA-DFT supercell calculations [82, 124]. There is also a transverse mode that strongly couples the equivalent sites in the (110) plane containing the B–H complex. The calculated mode is 1975 cm^{-1} [82, 124], and hence quantum mechanical tunnelling effects are very important. The deuterium modes have also been calculated at 1973 and 1530 cm^{-1} for ^{10}B, and there is a downward shift in frequency of around 0.3–0.4% with ^{11}B [82].

It is not clear whether these LVMs would be visible in IR absorption measurements, since they may either have a low effective charge or, perhaps more likely, they may couple with a reorientation about the B impurity.

6.2. Hydrogen–nitrogen complexes

Unlike the case for B-doped diamond, there is no evidence of hydrogenation of substitutional nitrogen in diamond [37].

Theoretically, hydrogen will bind to donors and passivate them in much the same way as it does acceptors. For example the phosphorus donor in silicon is passivated with hydrogen lying at the anti-bonding location AB2 [167], shown in figure 5. This can be understood quite simply in silicon since hydrogen adopts this location in the negative charge state. Since the acceptor site in diamond is likely to be the bond centre, it is therefore unsurprising that the nitrogen–hydrogen pair locates hydrogen at this site [145]. From semi-empirical calculations

the hydrogen atom lies closer to the carbon neighbour, with the overall N–H–C separation being dilated by around 0.26 Å relative to the already dilated N–C bond, with the C–H and N–H distances being 1.06 and 1.20 Å, respectively [145]. This structure was reproduced closely in LDA-DFT supercell calculations, with the C–H and N–H distances being 1.06 and 1.26 Å. The bond-centred configuration is 1.4 and 3.0 eV below the AB1 and AB2 sites, respectively [82].

In the semi-empirical cluster calculations [145] the binding energy of this structure was found to be 1.49 eV, presumably relative to neutral substitutional N and a hydrogen atom in vacuum. This is comparable to the binding energy of the boron–hydrogen pair calculated using the same approximations [145], and similar to the binding energy of the N–H defect found from LDA-DFT methods [82] at 4.2 and 3.5 eV for the reactions N–H $\rightarrow$ $N^0 + H^0$ and N–H $\rightarrow$ $N^+ + H^-$, respectively, assuming a formation energy of bond-centred hydrogen at 2.6 eV.

The complex possesses a filled level in the band gap, and therefore cannot be described as passivated from these calculations alone. LDA-DFT supercell calculations using substitutional nitrogen as a reference level (see section 2.7.3) places the donor level at $E_v + 1.1$ eV [82] and an *ab initio* formation energy approach (section 2.7.2) yields $E_v + 1.5$ eV [82]. Since the formation of the N–H defect requires isolated N and H, the Fermi level is unlikely ever to lead to an ionized N–H pair.

The motion of the H atom around substitutional nitrogen has been estimated at around 2.54 eV [145], with a trajectory similar to that previously found for isolated hydrogen, viz a direct hop between bond centres within a (110) plane. This, in conjunction with the relatively large migration barrier for neutral and negative bond-centred hydrogen, suggest that a N–H pair would be stable to reasonably high temperatures.

The defect has a calculated stretch mode at 3324 cm^{-1}, which drops by 6 and 910 cm^{-1} with ^{13}C and D, respectively [82]. The effect of replacing ^{14}N with ^{15}N has a negligible ($<$0.1 cm^{-1}) effect since the H atom is bonded to the C-atom and is more distant from the nitrogen. There is also a bend mode at 1400 cm^{-1}. This, along with the thermal stability, has led to a tentative assignment of the N–H defect to the 3107 cm^{-1} IR absorption peak or the 3124 cm^{-1} peak seen in CVD material.

Finally, a model structure involving hydrogen and nitrogen that gives rise to a shallow donor level was proposed [97]. This defect is made up from the A centre (a pair of nearest-neighbour nitrogen atoms) with a hydrogen atom placed in the bond centre between the two N atoms. The A-centre defect is a prime site for bond-centred hydrogen since it has a very long N–N separation comparable to the dilation seen when H lies between two carbon atoms. The dilation induced by the addition of the H to the A centre is just 3%. Using the substitutional N centre as an empirical marker, the N–H–N defect is calculated to yield a donor level at around $E_c - 0.6$ eV [97], i.e. comparable to substitutional phosphorus [168, 169]. The formation energy of the complex is calculated to be in the 4–5 eV range, and in particular the cost of the N–H–N defect is very close to VN, which is a very common defect in CVD material. The binding of the complex is just 2 eV, which might be a bigger issue than the solubility since it may be unstable at the growth temperature of CVD material. Furthermore, nitrogen is typically incorporated into CVD material as single N centres, either as substitutional N or complexes with a lattice vacancy, and the barrier to migration of substitutional N, as obtained from the activation energy for the aggregation into A centres, is 5 eV [170]. Perhaps a more attractive method for the formation of these centres is implantation of protons into type IaA material (i.e. where nitrogen is already in the A-centre aggregate form) followed by an anneal, but then one is competing with the formation of stable VN_2 and other nitrogen–vacancy complexes which would act as compensating centres. Furthermore, one would prefer to be doping CVD diamond for the production of p–n junctions and so on.

6.3. Hydrogen–phosphorus complexes

Phosphorus is a potential n-type dopant in diamond, although the donor level has been shown to lie around 0.6 eV below the conduction band [168, 169]. With such a deep level, phosphorus has a very small ionization fraction at room temperature and there is much work being performed to find a more shallow donor.

Density functional calculations show that H binds to phosphorus in an anti-bonding site [125, 140], bonded to the phosphorus atom (AB1, figure 5), rather than anti-bonding to a neighbouring host atom as is the case for the P–H pair in silicon [167]. The binding energy is estimated to be 2.56 eV [125, 140], 3.1 eV [82] and 2.45 eV [89] for dissociation into neutral components, and 1.0 eV [82] and 1.85 eV [89] for decomposition into charged components, P^+ and H^-. The difference in the latter two values is a reflection of the different estimates for the electrical levels of bond-centred hydrogen.

H in the bond centre is found to be 2.4 eV [125, 140] and 3.5 eV [82] higher in energy, with AB3 being higher in energy by around 1.2 eV [125, 140] or 1.5 eV [82]. AB2, the structure found in silicon, is 1.7 eV higher [82].

As with the N–H pair, the hydrogen acts as an acceptor and partially passivates the phosphorus donor, with the complex possessing a filled state in the band gap [82, 140]. This has been calculated to lead to a donor level at $E_c - 3.0$ eV [82] from LDA-DFT and $E_c - 3.29$ eV from GGA-DFT. One study suggested that the resultant defect also gives rise to an empty state very close to the conduction band minimum that might play a role in hopping conduction involving unpassivated phosphorus and P–H pairs [140]. However, such a process requires the pair to possess an acceptor level, which formation energy calculations do not find [82].

The AB1 structure is predicted to give rise to high frequency stretch and bend LVMs at 2668 and 1853 cm^{-1} [125, 140] using the harmonic approximation (section 2.7.4) but only considering motion of the H atom. Calculations taking the motion of all the atoms into account lead to stretch and bend modes much higher in frequency at 2985 and 2142 cm^{-1}, respectively, which are lowered to 2016 and 1537 cm^{-1} when H is replaced with D [82]. The effective charge of the oscillations are calculated to be relatively large and should be resolvable experimentally provided sufficient centres can be formed.

6.4. Hydrogen–sulfur complexes

Sulfur has recently attracted attention due to the suggestion that it can be used to form n-type diamond [171]. The reality of the effect is still controversial, with accidental boron contamination apparently responsible for some of the observations [172]. There are also inconsistencies in the theoretical location of the sulfur donor levels, with them lying either very close to the conduction band [88], or more likely being rather deep [89, 104, 140, 173]. The general consensus is that substitutional sulfur generates a donor level that is too deep for semiconductor applications, but that the interaction of other impurities, including hydrogen, may bring the donor level into a more accessible location.

The simple S–H pair is lowest in energy when H lies at the AB1 site [125, 140, 163] (figure 5), just as found with phosphorus. The BC and AB3 sites are predicted to be 0.78 and 1.22 eV higher in energy [125]. The binding energy of the pair in the neutral charge state is 2.56 eV from LDA-DFT supercell calculations [125, 140]. The $S–H_{AB}$ pair remains a deep donor in these calculations ($E_c - 1.07$ eV) and has LVMs at around 2787 and 1774 cm^{-1}, close to those found using the same approach for the P–H pair. The estimate of a deep donor level arises from the one-electron orbital energy, and as such is not a true evaluation of a donor level.

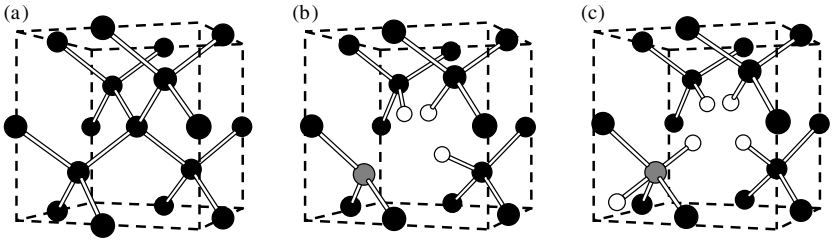

Figure 6. Schematic diagrams to illustrate the S–H–V complexes calculated to give rise to shallow donor levels [96, 163]. The black, grey and white atoms represent C, S and H, respectively. (b) SVH_3 and (c) SVH_4H_{AB}. (a) shows the corresponding section of defect-free material for comparison.

Using GGA-DFT methods, Miyazaki *et al* [96, 163] found that there are several forms of combinations of a sulfur, hydrogen and vacancy that generate *shallow* donors, with levels 0.5–0.6 eV below the conduction band minimum. In particular, and in contrast to Nishimatsu *et al* [125, 140], one of these centres is the H–S pair, but also SVH_3 and SVH_4H_{AB} are found to be shallow donors. The structures of the vacancy-related defects are shown schematically in figure 6. The evaluation of $S–H_{AB}$ as a *shallow* donor in contrast to Nishimatsu *et al* [125, 140] may be a reflection of the method of evaluation of the donor level, but in any case highlights the difficulty in obtaining unambiguous values for this type of quantity. $S–H_{AB}$ and SVH_4H_{AB} are isoelectronic and one would expect them to have qualitatively similar properties.

The main problems with these structures as dopants are the absolute formation energy (4 eV and greater) and more significantly the fact that alternative structures, such as vacancy–hydrogen complexes or even isolated hydrogen, are more stable for a wide range of hydrogen chemical potentials. Furthermore, there are many more structures with *deep* levels that can be formed from the same constituents, and under any thermally annealed conditions it seems unlikely that the beneficial complexes would survive.

As with phosphorus, an impurity band conduction model has been proposed, with S–H pairs supplying an electron to impurity bands from fully hydrogenated S [125, 140], but one should exercise caution given the discrepancies in the S–H donor levels between methods, and the doubt shed over the existence of an acceptor state for the analogous P–H complex.

7. Hydrogen and extended defects

The unexpectedly high concentrations of hydrogen in diamond has led to speculation that it is trapped in grain boundaries, voids or dislocations [11, 174]. Dislocations are found in CVD diamond originating from grain boundaries, internal twinning and from the substrate. Hence there are potentially regions containing considerable concentrations of either dangling or strained bonds. They therefore are a particularly attractive sink for hydrogen in the material. *Ab initio* cluster calculations have shown that the binding energy of bond-centred, neutral hydrogen to a neutral soliton or soliton–kink pair is as high as 4.8 and 5.3 eV, respectively [175]. Taking the energy of bond-centred hydrogen from section 3.5, the absolute formation energy of hydrogen at these sites is therefore either small or negative, strongly indicating dislocations as an equilibrium sink for hydrogen. The hydrogen also reduces the activation energy for the motion of 90° partial dislocations from 3.3 eV [176] to just 1.67 eV [175].

Hydrogen pairs at the single-period 90° partial dislocation form the di-bond-centred configuration shown in figure 3(c) rather than H_2^*, with an energy difference of 1.7 eV [82, 124]. In fact this is not at all surprising since the bonds at the core of a dislocation are strained and

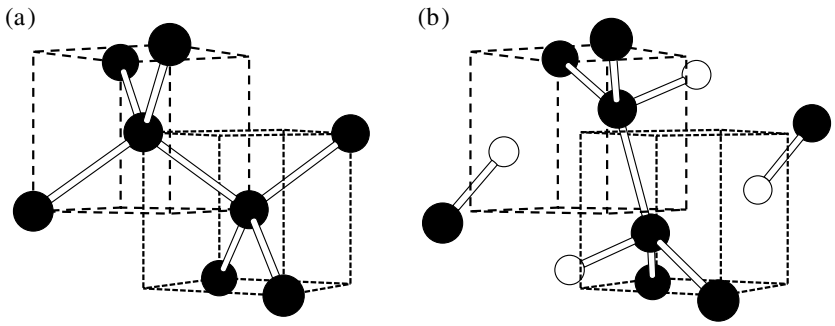

Figure 7. Schematic representation of (b) the dislocation dipole formed by the aggregation of four H atoms. The black and white circles represent C and H, respectively. (a) shows the corresponding section of defect-free material for comparison.

the presence of hydrogen pairs both relieves this strain and leaves the dislocation passive. The hydrogen dimer is bound by around 4 eV.

However, even if all the sites in dislocations in diamond were hydrogenated, it seems unlikely that this alone could account for the large concentrations of hydrogen in some samples.

More recently a model has been put forward for a complex of four hydrogen atoms that constitute a dislocation dipole [177]. The structure of the H_4 complex can be viewed as a pair of H_2^* defects in neighbouring bonds and is shown schematically in figure 7.

This structure is very stable and bound with respect to two H_2^* defects. The formation of this incipient dislocation dipole spontaneously upon the aggregation of just four H atoms is a potential low energy nucleation site for further hydrogen capture leading to extension of this defect.

Also studied are hydrogen atoms in the 'platelet' defects seen in silicon. In these defects a large area $\{111\}$ planar defect is formed by inserting pairs of hydrogen atoms into bulk bonds. For the case of silicon there is some debate regarding the nucleation and growth of these structures, and there appears to be various stages in the aggregation of hydrogen. There is no direct experimental evidence that these structures exist in diamond, but the presence of large concentrations of hydrogen in the subsurface region has implied an unidentified trapping site in this material. For 'infinite' hydrogen platelets, as modelled using periodic boundary conditions, the minimum formation energy per H atom is found to be large and *negative* [177]. This implies under equilibrium conditions that, in the presence of large concentrations of hydrogen, these structures should form. It is perhaps these large area defects that form the most energetically favourable sink for the large concentrations of hydrogen in diamond, although the nucleation and growth remains to be fully explored theoretically [177].

8. Concluding remarks

The theoretical treatment of hydrogen and muonium in diamond has spanned the last twenty years and provided a range of basic properties of hydrogen dissolved in diamond. These data are made all the more important than in some other materials since unambiguous experimental data are lacking in all but a small number of cases. Listed in this section are a selection of the principal conclusions taken from this review.

(i) The general result from theory is that isolated interstitial hydrogen is thermodynamically *insoluble* in bulk diamond. This equilibrium property should, however, be viewed in the

proper perspective. For example, using the same theoretical methods the formation energy of V–N and bond-centred hydrogen defects are 4–5 and 6 eV, respectively [97]. Therefore one would also expect V–N centres to be absent from CVD diamond, whereas it is well known that the characteristic optical centres at 1.945 and 2.156 eV arising from $(VN)^-$ and $(VN)^0$ are commonly detected in N-containing CVD samples. This might imply that the concentration of VN, and hence potentially that of H, is due to the incorporation processes at the growing surface and not dictated by the equilibrium thermodynamics.

(ii) The interaction of hydrogen with other defects in diamond often results in electrically active centres. Indeed the bond-centred hydrogen defect possesses both donor and acceptor levels deep in the band gap, and the partial passivation of sulfur may result in a shallow donor. However, the variability in the predicted electrical levels of defects means that caution must be exercised when interpreting total energy calculations. The interaction of H with P and S may be exploited in some way via a hopping conduction process and, provided the defect stability is sufficiently high, such co-doping techniques may have a role in the future development of n-type diamond.

(iii) Some C–H vibrations may be effectively IR-inactive, not on symmetry grounds, but instead due to a small effective charge. This effect has been observed in C–H vibrations from defects in silicon [178, 179]. This may go some way to explaining the gap between the amount of hydrogen believed to be present in the material by looking at the integrated intensity of C–H modes, and that seen using more destructive methods.

(iv) Bond-centred hydrogen migrates in diamond with an activation barrier between around 1.6 and 2.0 eV. However, positively charged interstitial hydrogen is much more mobile, linking very well with the B–D interactions seen experimentally. H_2^* hydrogen aggregates are much less mobile, as are vacancy–hydrogen complexes, suggesting that the complexing of hydrogen in many cases may have a pinning effect on other defects.

(v) Hydrogen is relatively strongly bound to almost all defects in diamond. It binds to donors and acceptors, lattice vacancies and dislocations with energies of the order of several electronvolts. The formation of internal surfaces or platelets is exothermic, and aggregates of just four hydrogen atoms are sufficient for the spontaneous nucleation of a dislocation dipole. This may have implications for the large subsurface concentrations of hydrogen in plasma-treated samples.

(vi) The calculation of the hyperfine terms associated with muonium and H-related EPR is a far from trivial matter with apparently similar methods giving very different values. However, the values for the H1/H2 EPR centre are close to those predicted for V–H defects, and although it is far from clear that a correlation can be drawn, this leads to interesting questions regarding other vacancy–hydrogen defects including their optical and electrical activity and their thermal stability, since if these centres are present in CVD material they might well impact on electronic and optical device applications.

With the emergence of CVD diamond as a viable electronic material the understanding of the role of H in defect formation and passivation is sure to attract a great deal of interest in the future and it is likely that theoretical modelling will be at the centre of this work.

Acknowledgments

I would like to acknowledge Patrick Briddon, Malcolm Heggie, Chris Ewels, Ben Hourahine, Alexander Blumenau and Bob Jones for helpful comments during the preparation of this review.

References

[1] Pearton S J, Corbett J W and Stavola M 1992 *Hydrogen in Crystalline Semiconductors* (Berlin: Springer) ch 3
[2] Myers S M, Baskes M I, Birnbaum H K, Corbett J W, Deleo G G, Estreicher S K, Haller E E, Jena P, Johnson N M, Kirchheim R, Pearton S J and Stavola M J 1992 *Rev. Mod. Phys.* **64** 559–617
[3] Estreicher S K 1995 *Mater. Sci. Eng.* R **14** 319–412
[4] Van de Walle C G 1998 *J. Vac. Sci. Technol.* A **16** 1767–71
[5] Nickel N H (ed) 1999 Hydrogen in semiconductors II *Semiconductors and Semimetals* vol 61 (New York: Academic)
[6] Stavola M 1999 *Properties of Crystalline Silicon (EMIS Datareviews Series No 20)* ed R Hull (London: INSPEC, Institute of Electrical Engineers) ch 9.8 pp 511–21
[7] Stavola M 1999 *Properties of Crystalline Silicon (EMIS Datareviews Series No 20)* ed R Hull (London: INSPEC, Institute of Electrical Engineers) ch 9.9. pp 522–37
[8] Jones R, Coomer B J, Goss J P, Hourahine B and Resende A 2000 *Solid State Phenom.* **71** 173–248
[9] Isberg J, Hammersberg J, Johansson E, Wikström T, Twitchen D J, Whitehead A J, Coe S E and Scarsbrook G A 2002 *Science* **297** 1670–2
[10] Sellschop J P F, Annegarn H J, Madiba C, Keddy R J and Renan M J 1977 *Ind. Diamond Rev. Sup.* 2–4
[11] Dischler B, Wild C, Müller-Sebert W and Koidl P 1993 *Physica* B **185** 217–21
[12] Holzschuh E, Kündig W, Meier P F, Patterson B D, Sellschop J P F, Stemmet M C and Appel H 1982 *Phys. Rev.* A **25** 1272–86
[13] Patterson B D, Hintermann A, Kündig W, Meier P F, Waldner F, Graf H, Recknagel E, Weidinger A and Wichert T 1978 *Phys. Rev. Lett.* **40** 1347–450
[14] Holzschuh E, Graf H, Recknagel E, Weidinger A, Wichert T and Meier P F 1979 *Phys. Rev.* B **20** 4391–6
[15] Wang J S and Kittel C 1973 *Phys. Rev.* B **7** 713–18
[16] Watanabe I and Sugata K 1988 *Japan. J. Appl. Phys.* **27** 1808–11
[17] Jia H, Shinar J, Land D P and Pruski M 1993 *Phys. Rev.* B **48** 17595–8
[18] Holder S L, Rowan L G and Krebs J J 1994 *Appl. Phys. Lett.* **64** 1091–3
[19] Zhou X, Watkins G D and McNamara Rutledge K M 1995 *Mater. Sci. Forum* **196–201** 825–30
[20] Zhou X, Watkins G D, McNamara Rutledge K M, Messmer R P and Chawla S 1996 *Phys. Rev.* B **54** 7881–90
[21] Nistor S V, Stefan M, Ralchenko V, Khomich A and Schoemaker D 2000 *J. Appl. Phys.* **87** 8741–6
[22] Talbot-Ponsonby D F, Newton M E, Baker J M, Scarsbrook G A, Sussmann R S, Whitehead A J and Pfenninger S 1998 *Phys. Rev.* B **57** 2264–70
[23] Rosa J, Pangrác J, Vaněček M, Vorlíček V, Nesládek M, Meykens K, Quaeyhaegens C and Stals L M 1998 *Diamond Relat. Mater.* **7** 1048–53
[24] Iakoubovskii K, Stesmans A, Suzuki K, Sawabe A and Yamada T 2002 *Phys. Rev.* B **66** 113203
[25] Iakoubovskii K and Stesmans A 2002 *Phys. Rev.* B **66** 195207
[26] McNamara K, Williams B, Gleason K and Scruggs B E 1994 *J. Appl. Phys.* **76** 2466–72
[27] Davies G, Collins A T and Spear P 1984 *Solid State Commun.* **49** 433–6
[28] Fuchs F, Wild C, Schwarz K, Müller-Sebert W and Koidl P 1995 *Appl. Phys. Lett.* **66** 177–9
[29] Runciman W A and Carter T 1971 *Solid State Commun.* **9** 315–17
[30] Kiflawi I, Fisher D, Kanda H and Sittas G 1996 *Diamond Relat. Mater.* **5** 1516–18
[31] De Weerdt F and Kupriyanov I N 2002 *Diamond Relat. Mater.* **11** 714–15
[32] Chevallier J, Theys B, Lusson A, Grattepain C, Deneuville A and Gheeraert E 1998 *Phys. Rev.* B **58** 7966–9
[33] Chevallier J, Ballutaud D, Theys B, Jomard F, Deneuville A, Gheeraert E and Pruvost F 1999 *Phys. Status Solidi* a **174** 73–81
[34] Zeisel R, Nebel C E and Stutzmann M 1999 *Appl. Phys. Lett.* **74** 1875–6
[35] Ballutaud D, Jomard F, Le Duigou J, Theys B, Chevallier J, Deneuville A and Pruvost F 2000 *Diamond Relat. Mater.* **9** 1171–4
[36] Chevallier J, Lusson A, Ballutaud D, Theys B, Jomard F, Deneuville A, Bernard M, Gheeraert E and Bustarret E 2001 *Diamond Relat. Mater.* **10** 399–404
[37] Chevallier J, Jomard F, Teukam Z, Koizumi S, Kanda H, Sato Y, Deneuville A and Bernard M 2002 *Diamond Relat. Mater.* **11** 1566–71
[38] Hayashi K, Watanabe H, Yamanaka S, Sekiguchi T, Okushi H and Kajimura K 1997 *Diamond Relat. Mater.* **3** 303–7
[39] Looi H J, Jackman R B and Foord J S 1998 *Appl. Phys. Lett.* **72** 353–5
[40] Looi H J, Pang L Y S, Malloy A B, Jones F, Whitfield M D, Foord J S and Jackman R B 1999 *Carbon* **37** 801–5
[41] Jackman R B, Looi H J, Pang L Y S, Whitfield M D and Foord J S 1999 *Carbon* **37** 817–22

[42] Smith S D and Taylor W 1961 *Proc. R. Soc.* **73** 1142
[43] Sze S M 1981 *Physics of Semiconductor Devices* 2nd edn (New York: Wiley)
[44] Singh J 1993 *Physics of Semiconductors and Their Heterostructures* (New York: McGraw-Hill)
[45] Collins A T and Williams A W S 1971 *J. Phys. C: Solid State Phys.* **4** 1789–800
[46] Szaneitat M, Jiang X and Beyer W 2000 *Appl. Phys. Lett.* **77** 1554–6
[47] Williams O A, Whitfield M D, Jackman R B, Foord J S, Butler J E and Nebel C E 2001 *Appl. Phys. Lett.* **78** 3460–2
[48] Williams O A, Whitfield M D, Jackman R B, Foord J S, Butler J E and Nebel C E 2001 *Diamond Relat. Mater.* **10** 423–8
[49] Sauerer C, Ertl F, Nebel C E, Stutzmann M, Bergonzo P, Williams O A and Jackman R A 2001 *Phys. Status Solidi* A **186** 241–7
[50] Nebel C E, Sauerer C, Ertl F, Stutzmann M, Graeff C F O, Bergonzo P, Williams O A and Jackman R 2001 *Appl. Phys. Lett.* **79** 4541–3
[51] Ri S G, Mizumasa T, Akiba Y, Hirose Y, Kurosu T and Iida M 1995 *Japan. J. Appl. Phys.* **34** 5550–5
[52] Maier F, Riedel F, Mantel B, Ristein J and Ley L 2000 *Phys. Rev. Lett.* **85** 3472–5
[53] Ristein J, Maier F, Riedel M, Stammer M and Ley L 2001 *Diamond Relat. Mater.* **10** 416–22
[54] Hayashi K, Watanabe H, Yamanaka S, Okushi H, Kajimura K and Sekiguchi T 1996 *Appl. Phys. Lett.* **69** 1122–4
[55] Iakoubovskii K and Stesmans A 2002 *J. Phys.: Condens. Matter* **14** R467–99
[56] Nazaré M H 1994 *Properties and Growth of Diamond (EMIS Datareviews Series No 9)* ed G Davies (London: INSPEC, Institute of Electrical Engineers) ch 4.1 pp 129–32
[57] Neves A J and Lopes J C 2001 *Properties, Growth and Applications of Diamond (EMIS Datareviews Series No 26)* ed M H Nazaré and A J Neves (London: INSPEC, Institute of Electrical Engineers) ch A6.1 pp 167–71
[58] Zaitsev A M 2001 *Properties, Growth and Applications of Diamond (EMIS Datareviews Series No 26)* ed M H Nazaré and A J Neves (London: INSPEC, Institute of Electrical Engineers) ch A5.7 pp 155–62
[59] Iakoubovskii K and Adriaenssens G J 2000 *Phys. Rev.* B **61** 10174–82
[60] Pickett W E 1989 *Comput. Phys. Rep.* **9** 115–97
[61] Halgren T A and Lipscomb W N 1973 *J. Chem. Phys.* **58** 1569–91
[62] Marynick D S and Lipscomb W N 1982 *Proc. Natl Acad. Sci. USA* **79** 1341–5
[63] Pople J A and Beverage D L 1970 *Approximate Molecular Orbital Theory* (New York: McGraw-Hill)
[64] Deák P 1999 *Properties of Crystalline Silicon (EMIS Datareviews Series No 20)* ed R Hull (London: INSPEC, Institute of Electrical Engineers) ch 6.1 pp 245–56
[65] Hohenberg P and Kohn W 1964 *Phys. Rev.* **136** B864–71
[66] Kohn W and Sham L J 1965 *Phys. Rev.* **140** A1133–8
[67] Jones R O and Gunnarsson O 1989 *Rev. Mod. Phys.* **61** 689–743
[68] Dreizler R M and Gross E K U 1990 *Density Functional Theory* (Berlin: Springer)
[69] Dobson J F, Das M P and Vignale G (ed) 1998 *Electronic Density Functional Theory: Recent Progress and New Directions* (New York: Kluwer–Academic)
[70] Jones R and Briddon P R 1998 The *ab initio* cluster method and the dynamics of defects in semiconductors *Semiconductors and Semimetals* vol 51A (Boston, MA: Academic) ch 6
[71] Joubert D (ed) 1999 *Density Functionals: Theory and Application (Springer Lecture Notes in Physics vol 500)* (New York: Springer)
[72] Rauls E, Lingner T, Hajnal Z, Greulich-Weber S, Frauenheim T and Spaeth J M 2000 *Phys. Status Solidi* b **217** R1–3
[73] Blumenau A T, Heggie M I, Fall C J, Jones R and Frauenheim T 2002 *Phys. Rev.* B **65** 205205
[74] Zapol P, Sternberg M, Curtiss L, Frauenheim T and Gruen D 2002 *Phys. Rev.* B **65** 045403
[75] Jungnickel G 1999 *Properties of Crystalline Silicon (EMIS Datareviews Series No 20)* ed R Hull (London: INSPEC, Institute of Electrical Engineers) ch 6.2 pp 257–66
[76] Monkhorst H J and Pack J D 1976 *Phys. Rev.* B **13** 5188–92
[77] Blochl P E, Van de Walle C G and Pantelides S T 1990 *Phys. Rev. Lett.* **64** 1401–4
[78] Forsythe K M and Makri N 1998 *J. Chem. Phys.* **108** 6819–28
[79] Forsythe K M and Makri N 1999 *J. Chem. Phys.* **110** 6082
[80] Miyake T, Ogitsu T and Tsuneyuki S 1999 *Phys. Rev.* B **60** 14197–204
[81] Estreicher S K, Wells K, Fedders P A and Ordejón P 2001 *J. Phys.: Condens. Matter* **13** 6271–83
[82] Goss J P, Jones R, Heggie M I, Ewels C P, Briddon P R and Öberg S 2002 *Phys. Rev.* B **65** 115207
[83] Goss J P, Jones R, Breuer S J, Briddon P R and Öberg S 1996 *Phys. Rev. Lett.* **77** 3041–4
[84] Briddon P R and Jones R 1993 *Physica* B **185** 179–89

[85] Goss J P, Coomer B J, Jones R, Shaw T D, Briddon P R, Rayson M and Öberg S 2001 *Phys. Rev.* B **63** 195208
[86] Goss J P, Coomer B J, Jones R, Fall C J, Latham C D, Briddon P R and Öberg S 2000 *J. Phys.: Condens. Matter* **12** 10257–61
[87] Gerstmann U, Amkreutz M and Overhof H 2000 *Phys. Status Solidi* b **217** 665–84
[88] Saada D, Adler J and Kalish R 2000 *Appl. Phys. Lett.* **77** 878–9
[89] Wang L G and Zunger A 2002 *Phys. Rev.* B **66** 161202
[90] Breuer S J and Briddon P R 1995 *Phys. Rev.* B **51** 6984–94
[91] Breuer S J and Briddon P R 1996 *Phys. Rev.* B **53** 7819–22
[92] Goss J P, Jones R and Briddon P R 2002 *Phys. Rev.* B **65** 035203
[93] Makov G and Payne M C 1995 *Phys. Rev.* B **51** 4014–122
[94] Lannoo M and Bourgoin J 1981 Point defects in semiconductors I *Solid-State Sciences* (Berlin: Springer)
[95] Lento J, Mozos J L and Nieminen R M 2002 *J. Phys.: Condens. Matter* **14** 2637–46
[96] Miyazaki T and Okushi H 2002 *Diamond Relat. Mater.* **11** 323–7
[97] Miyazaki T, Okushi H and Uda T 2002 *Phys. Rev. Lett.* **88** 066402
[98] Lide D R (ed) 1996 *CRC Handbook of Chemistry and Physics* 77th edn (Boca Raton, FL: Chemical Rubber Company Press)
[99] Watkins G D and Corbett J W 1961 *Phys. Rev.* **121** 1001–14
[100] Pesola M, von Boehm J, Mattila T and Nieminen R M 1999 *Phys. Rev.* B **60** 11449–63
[101] Resende A, Jones R, Öberg S and Briddon P R 1999 *Phys. Rev. Lett.* **82** 2111–14
[102] Coutinho J, Torres V J B, Jones R and Briddon P R 2003 *Phys. Rev.* B **67** 035205
[103] Jeong J W and Oshiyama A 2001 *Phys. Rev.* B **64** 235204
[104] Albu T V, Anderson A B and Angus J C 2002 *J. Electrochem. Soc.* **149** E143–7
[105] Pruneda J M, Estreicher S K, Junquera J, Ferrer J and Ordejón P 2002 *Phys. Rev.* B **65** 075210
[106] Kiflawi I, Mainwood A, Kanda H and Fisher D 1996 *Phys. Rev.* B **54** 16719–26
[107] Goss J P, Jones R, Öberg S and Briddon P R 1997 *Phys. Rev.* B **55** 15576–80
[108] Clerjaud B and Côte D 1992 *J. Phys.: Condens. Matter* **4** 9919–26
[109] Odermatt W, Baumeler H P, Keller H, Kündig W, Patterson B D, Schneider J W, Sellschop J P F, Stemmet M C, Connell S and Spencer D P 1988 *Phys. Rev.* B **38** 4388–93
[110] Schreckenbach G and Zeigler T 1997 *J. Phys. Chem.* A **101** 3388–99
[111] Pickard C and Mauri F 2001 *Phys. Rev.* B **63** 245101
[112] Pickard C and Mauri F 2002 *Phys. Rev. Lett.* **88** 086403
[113] Brewer J H, Crowe K M, Gygax F N, Johnson R F, Patterson B D, Fleming D G and Schenck A 1973 *Phys. Rev. Lett.* **31** 143–6
[114] Sahoo N, Mishra S K, Mishra K C, Coker A, Das T P, Mitra C K, Snyder L C and Glodeanu A 1983 *Phys. Rev. Lett.* **50** 913–17
[115] Mainwood A and Stoneham A M 1984 *J. Phys. C: Solid State Phys.* **17** 2513–24
[116] Estreicher S, Ray A K, Fry J L and Marynick D S 1985 *Phys. Rev. Lett.* **55** 1976–8
[117] Claxton T A, Evans A and Symons M C R 1986 *J. Chem. Soc. Faraday Trans.* **82** 2031–7
[118] Estle T L, Estreicher S and Marynick D S 1986 *Hyperfine Interact.* **32** 637–9
[119] Estreicher S, Ray A K, Fry J L and Marynick D S 1986 *Phys. Rev.* B **34** 6071–9
[120] Estle T L, Estreicher S and Marynick D S 1987 *Phys. Rev. Lett.* **58** 1547–50
[121] Briddon P R, Jones R and Lister G M S 1988 *J. Phys. C: Solid State Phys.* **21** L1027–31
[122] Kaukonen M, Peräjoki J, Nieminen R M, Jungnickel G and Frauenheim T 2000 *Phys. Rev.* B **61** 980–7
[123] Saada D, Adler J and Kalish R 2000 *Phys. Rev.* B **61** 10711–15
[124] Goss J P, Jones R, Heggie M I, Ewels C P, Briddon P R and Öberg S 2001 *Phys. Status Solidi* a **186** 263–8
[125] Nishimatsu T, Katayama-Yoshida H and Orita N 2002 *Japan. J. Appl. Phys.* 1 **41** 1952–62
[126] Cox S F J and Symons M C R 1986 *Chem. Phys. Lett.* **126** 516–25
[127] Estreicher S K, Roberson M A and Maric D M 1994 *Phys. Rev.* B **50** 17018–27
[128] Bendazzoli G L and Donzelli O 1989 *J. Phys.: Condens. Matter* **1** 8227–34
[129] Vogel S, Celio M, Maric D J M and Meier P F 1989 *J. Phys.: Condens. Matter* **1** 4729–34
[130] Mehandru S P, Anderson A B and Angus J C 1992 *J. Mater. Res.* **7** 689–95
[131] Paschedag N, Suter H U, Maric D J M and Meier P F 1993 *Phys. Rev. Lett.* **70** 154–7
[132] Kanai C, Shichibu Y, Watanabe K and Takakuwa Y 2002 *Phys. Rev.* B **65** 153312
[133] Hoshiharu T, Asada T and Terakura K 1989 *Phys. Rev.* B **39** 5468–71
[134] Chawla S and Messmer R P 1996 *Appl. Phys. Lett.* **69** 3251–3
[135] Johnson N M, Herring C and Van de Walle C G 1994 *Phys. Rev. Lett.* **73** 130–3
[136] Seager C H, Anderson R A and Estreicher S K 1995 *Phys. Rev. Lett.* **74** 4565–5

[137] Hitti B, Kreitzman S R, Estle T L, Bates E S, Dawdy M R, Head T L and Lichti R L 1999 *Phys. Rev.* B **59** 4918–24
[138] Herring C, Johnson N M and Van de Walle C G 2001 *Phys. Rev.* B **64** 125209
[139] Kiliç Ç and Zunger A 2002 *Appl. Phys. Lett.* **81** 73–5
[140] Nishimatsu T, Katayama-Yoshida H and Orita N 2001 *Physica* B **302/303** 149–54
[141] Budde M 1998 Hydrogen-related defects in proton implanted silicon and germanium *PhD Thesis* Aarhus Center for Atomic Physics, University of Aarhus, Denmark
[142] Budde M, Cheney C P, Lupke G, Tolk N H and Feldman L C 2001 *Phys. Rev.* B **63** 195203
[143] Van de Walle C G, Denteneer P J H, Bar-Yam Y and Pantelides S T 1989 *Phys. Rev.* B **39** 10791–808
[144] Chu C H and Estreicher S K 1990 *Phys. Rev.* B **42** 9486–95
[145] Mehandru S P and Anderson A B 1994 *J. Mater. Res.* **9** 383–95
[146] Northrup J E, Di Felice R and Neugebauer J 1997 *Phys. Rev.* B **56** R4325–8
[147] Aradi B, Gali A, Deák P, Lowther J E, Son N T, Janzén E and Choyke W J 2001 *Phys. Rev.* B 245202
[148] Chen E E, Stavola M, Beall Fowler W and Walters P 2002 *Phys. Rev. Lett.* **88** 105507
[149] Chen E E, Stavola M, Beall Fowler W and Zhou J A 2002 *Phys. Rev. Lett.* **88** 245503
[150] Holbech J D, Bech Nielsen B, Jones R, Sitch P and Öberg S 1993 *Phys. Rev. Lett.* **71** 875–8
[151] Doyle B P, Maclear R D, Connell S H, Formenti P, Machi I Z, Butler J E, Schaaff P, Sellschop J P F, Sideras-Haddad E and Bharuth-Ram K 1997 *Nucl. Instrum. Methods* B **130** 204–10
[152] Bech Nielsen B, Hoffmann L and Budde M 1996 *Mater. Sci. Eng.* B **36** 259–63
[153] Xie L M, Qi M W and Chen J M 1991 *J. Phys.: Condens. Matter* **3** 8519–28
[154] Bech Nielsen B, Johannesen P, Stallinga P, Bonde Nielsen K and Byberg J R 1997 *Phys. Rev. Lett.* **79** 1507–10
[155] Stallinga P, Johannesen P, Herstrøm S, Bonde Nielsen K, Bech Nielsen B and Byberg J R 1998 *Phys. Rev.* B **58** 3842–52
[156] Xu H 1992 *Phys. Rev.* B **46** 1403–22
[157] Roberson M A and Estreicher S K 1994 *Phys. Rev.* B **49** 17040–9
[158] Park Y K, Estreicher S K, Myles C W and Fedders P A 1995 *Phys. Rev.* B **52** 1718–23
[159] Bech Nielsen B, Hoffmann L, Budde M, Jones R, Goss J and Öberg S 1995 *Mater. Sci. Forum* **196/201** 933–7
[160] Hastings J L, Gharaibeh M, Estreicher S K and Fedders P A 1999 *Physica* B **273/274** 216–19
[161] Lawson S C, Davies G, Collins A T and Mainwood A 1992 *J. Phys.: Condens. Matter* **4** 3439–52
[162] Mita Y 1996 *Phys. Rev.* B **53** 11360–4
[163] Miyazaki T, Okushi H and Uda T 2001 *Appl. Phys. Lett.* **78** 3977–9
[164] Bech Nielsen B, Andersen J U and Pearton S J 1988 *Phys. Rev. Lett.* **60** 321–4
[165] Denteneer P J H, Van de Walle C G and Pantelides S T 1989 *Phys. Rev. Lett.* **62** 1884–7
[166] Breuer S J and Briddon P R 1994 *Phys. Rev.* B **49** 10332–6
[167] Chang K J and Chadi D J 1988 *Phys. Rev. Lett.* **60** 1422–5
[168] Sternschulte H, Thonke K, Sauer R and Koizumi S 1999 *Phys. Rev.* B **59** 12924–7
[169] Nesládek M, Meykens K, Haenen K, Stals L M, Teraji T and Koizumi S 1999 *Phys. Rev.* B **59** 14852–5
[170] Evans T and Qi Z 1982 *Proc. R. Soc.* A **381** 159–78
[171] Sakaguchi I, N-Gamo M, Kikuchi Y, Haneda H, Suzuki T and Ando T 1999 *Phys. Rev.* B **60** 2139–41
[172] Kalish R, Reznik A, Uzan-Saguy C and Cytermann C 2000 *Appl. Phys. Lett.* **76** 757–9
[173] Miyazaki T and Okushi H 2001 *Diamond Relat. Mater.* **10** 449–52
[174] Seal M 1966 *Nature* **212** 1528–30
[175] Heggie M I, Jenkins S, Ewels C P, Jemmer P, Jones R and Briddon P R 2000 *J. Phys.: Condens. Matter* **12** 10263–70
[176] Sitch P K, Jones R, Öberg S and Heggie M I 1997 *J. Physique* III **7** 1381–7
[177] Heggie M I, Ewels C P, Martsinovich N, Scarle S, Jones R, Goss J P, Hourahine B and Briddon P R 2002 *J. Phys.: Condens. Matter* **14** 12689–96
[178] Pajot B, Clerjaud B and Xu Z J 1999 *Phys. Rev.* B **59** 7500–6
[179] Markevich V P, Murin L I, Hermansson J, Kleverman M, Lindström J L, Fukata N and Suezawa M 2001 *Physica* B **302/303** 220–6